

RADIATIVE KAON DECAYS AND THE PENGUIN CONTRIBUTION TO THE $\Delta I = 1/2$ RULE

JEAN-MARC GÉRARD,¹ CHRISTOPHER SMITH,² and STÉPHANIE TRINE²

¹ *Institut de Physique Théorique, Université catholique de Louvain,
Chemin du Cyclotron 2, B-1348 Louvain-la-Neuve, Belgium*

² *INFN, Laboratori Nazionali di Frascati, Via E. Fermi 40, I-00044 Frascati, Italy*

Abstract

A consistent census of penguins in the $\Delta I = 1/2$ rule is taken from the η_0 pole contribution to the radiative $K_L \rightarrow \gamma\gamma$, $K_S \rightarrow \pi^0\gamma\gamma$ and $K^+ \rightarrow \pi^+\gamma\gamma$ decay modes. We briefly comment on its impact for $K_L \rightarrow \pi^0\pi^0\gamma\gamma$, $K_L \rightarrow \pi^+\pi^-\gamma$ and check its compatibility with the $K_L - K_S$ mass difference and the CP violating ε'/ε parameter.

1 Introduction

A precise quantitative understanding of hadronic kaon decays has, up to now, been upset by the non-perturbative nature of strong interactions at low energy. Though qualitatively, there is little doubt that the $\Delta I = 1/2$ rule is a pure QCD effect, the genuine mechanism still eludes us. In particular, the relative strength of penguin and current-current operators has been debated for years. This has in turn impeded theorists from making use of the remarkable precision achieved in ε'/ε measurements.

In the present work, this question is addressed from a phenomenological point of view. The relative contribution of penguin and current-current operators in the $\Delta I = 1/2$ rule is known to be accessible from anomaly-driven radiative K decays, i.e. decays occurring through π, η, η' poles. Still, a thorough investigation in the context of large- N_c Chiral Perturbation Theory (ChPT) is called for. In particular, we will see that $U(3)$ ChPT holds the key to understand, and go beyond, the well-known vanishing of the $SU(3)$ $K_L \rightarrow \gamma\gamma$ amplitude at lowest order. Besides, the experimental situation has been improved and is expected to continue doing so for a number of radiative K decays. It is thus appropriate to review their theoretical treatment, especially regarding η_0 effects, and to guide experimentalists towards suitable observables to probe the $\Delta I = 1/2$ rule.

The paper is organized as follows. In the first section, the large- N_c formalism is recalled, with emphasis on the $U(3)$ ChPT weak operator basis. In particular, the strategy to extract the penguin fraction from phenomenology is exposed. The next few sections deal with radiative K decays. We first review in great details the $K_L \rightarrow \gamma\gamma$ mode, and develop the phenomenological tools to deal with $\eta - \eta'$ mixing to be used in the rest of the paper. Then we go on with the $K_S \rightarrow \pi^0\gamma\gamma$ decay and the pole contribution to the $K^+ \rightarrow \pi^+\gamma\gamma$ one, which are both quite sensitive to $\eta - \eta'$ effects. The $K_L \rightarrow \pi^0\pi^0\gamma\gamma$ and $K_L \rightarrow \pi^+\pi^-\gamma$ modes are only briefly analyzed as no new information can be obtained from them. Finally, the implications for the hadronic observables ΔM_{LS} and ε'/ε are investigated. Our results are summarized in the conclusion.

In the appendix, the complete analysis of $K_L \rightarrow \gamma\gamma$ in $SU(3)$ at $\mathcal{O}(p^6)$ is presented, some aspects of which are used throughout the paper to investigate the reduction of $U(3)$ amplitudes to $SU(3)$ ones.

2 Theoretical framework

Our starting point is the QCD-induced $\Delta S = 1$ effective weak Hamiltonian below the charm mass scale [1, 2]:

$$\mathcal{H}_{eff}^{\Delta S=1}(\mu < m_c) = \frac{G_F}{\sqrt{2}} V_{ud} V_{us}^* \sum_{i=1}^6 \left[z_i(\mu) - \frac{V_{td} V_{ts}^*}{V_{ud} V_{us}^*} y_i(\mu) \right] Q_i \quad (1)$$

with the familiar current-current ($i = 1, 2$) and penguin ($i = 3, \dots, 6$) operators

$$\begin{aligned} Q_1 &= 4(\bar{s}_L \gamma_\alpha d_L)(\bar{u}_L \gamma^\alpha u_L), & Q_2 &= 4(\bar{s}_L \gamma_\alpha u_L)(\bar{u}_L \gamma^\alpha d_L), \\ Q_3 &= 4(\bar{s}_L \gamma_\alpha d_L)(\bar{q}_L \gamma^\alpha q_L), & Q_4 &= 4(\bar{s}_L \gamma_\alpha q_L)(\bar{q}_L \gamma^\alpha d_L), \\ Q_5 &= 4(\bar{s}_L \gamma_\alpha d_L)(\bar{q}_R \gamma^\alpha q_R), & Q_6 &= -8(\bar{s}_L q_R)(\bar{q}_R d_L), \end{aligned} \quad (2)$$

after Fierz reorderings. In our notations, $q_L^R \equiv \frac{1}{2}(1 \pm \gamma_5)q$ and the light flavors $q = u, d, s$ are summed over. The connection between Eq.(1) and kaon phenomenology requires of course

additional tools, QCD perturbation theory being helpless to estimate the Q_i hadronic matrix elements. We will make use of chiral Lagrangian techniques, as we now describe.

2.1 $U(3)$ chiral representation of $\Delta S = 1$ weak operators

As is well-known, the above operators are not all independent. Indeed, we have the identity

$$Q_2 - Q_1 = Q_4 - Q_3. \quad (3)$$

Besides, Q_4 and Q_6 have the same color and flavor structures. The chiral realization of the effective Hamiltonian $\mathcal{H}_{eff}^{\Delta S=1}$ must thus allow for an explicit representation of the left-handed flavor-singlet current in Q_3 if we want to be in a position to disentangle $Q_{1,2}$ and Q_6 contributions to the $\Delta I = 1/2$ kaon decay amplitudes. For this reason, we will perform the hadronization of Eq.(1) in the $U(3)$ chiral expansion, with an explicit flavor-singlet degree of freedom η_0 , rather than in $SU(3)$.

The extension of $SU(3)$ to $U(3)$ proceeds through the large- N_c limit, with N_c the number of QCD colors. Considering N_c as large is the key to a consistent disposal of the QCD $U(1)_A$ anomaly [3]. The spontaneous symmetry breaking $U(3)_L \times U(3)_R \rightarrow U(3)_V$ gives then rise to a nonet of pseudoscalar Goldstone bosons, which are written

$$U \equiv \exp i \frac{\sqrt{2}}{F} \begin{pmatrix} \frac{\pi^0}{\sqrt{2}} + \frac{\eta_8}{\sqrt{6}} + \frac{\eta_0}{\sqrt{3}} & & \pi^+ & & K^+ \\ & \pi^- & & -\frac{\pi^0}{\sqrt{2}} + \frac{\eta_8}{\sqrt{6}} + \frac{\eta_0}{\sqrt{3}} & K^0 \\ & & K^- & & \bar{K}^0 \\ & & & & -\frac{2\eta_8}{\sqrt{6}} + \frac{\eta_0}{\sqrt{3}} \end{pmatrix} \quad (4)$$

in the exponential parametrization. The anomalous breaking of the $U(1)_A$ symmetry is reintroduced through $1/N_c$ corrections. In particular, the leading nonlinear Lagrangian reads [4]

$$\mathcal{L}_S^{(p^2, \infty) + (p^0, 1/N_c)} = \frac{F^2}{4} \langle \partial_\mu U \partial^\mu U^\dagger \rangle + \frac{F^2}{4} \langle \chi U^\dagger + U \chi^\dagger \rangle + \frac{F^2}{16N_c} m_0^2 \langle \ln U - \ln U^\dagger \rangle^2 \quad (5)$$

where $\langle \rangle$ denotes a trace over flavors, the external source χ is frozen at $\chi = rM$ to account for meson masses, $M = \text{diag}(m_u, m_d, m_s)$ is the light quark mass matrix and m_0 represents the anomalous part of the η_0 mass. The ChPT symmetry-breaking scale F is identified with the neutral pion decay constant $F_\pi = 92.4$ MeV at this order. Note that the leading $SU(3)$ chiral Lagrangian is recovered in the limit $m_0 \rightarrow \infty$, when the η_0 decouples.

The effective Hamiltonian (1) contains both $(8_L, 1_R)$ and $(27_L, 1_R)$ representations of the chiral group $U(3)_L \times U(3)_R$. At leading order in the momentum expansion, four operators built out of U and χ have either of these transformation properties and at most one factorized η_0 field¹:

$$\begin{aligned} Q_8 &= 4(L_\mu L^\mu)_{23}, & Q_8^s &= 4(L_\mu)_{23} \langle L^\mu \rangle, & Q_8^m &= F^4 (\chi U^\dagger + U \chi^\dagger)_{23}, \\ Q_{27} &= 4 \left[(L_\mu)_{23} (L^\mu)_{11} + \frac{2}{3} (L_\mu)_{13} (L^\mu)_{21} - \frac{1}{3} (L_\mu)_{23} \langle L^\mu \rangle \right], \end{aligned} \quad (6)$$

where the matrix L_μ collects the chiral realizations of the left-handed currents from Eq.(5):

$$\bar{q}_L^k \gamma_\mu q_L^l \rightarrow i \frac{F^2}{2} \left(\partial_\mu U U^\dagger \right)^{lk} \equiv (L_\mu)^{lk} \quad (q^{l,k} = u, d, s). \quad (7)$$

¹Operators with two or more η_0 factors have negligible effects on the processes we will consider due to isospin, loop and/or $1/N_c$ suppressions.

Q_8 , Q_8^m and Q_{27} are the trivial $U(3)$ generalizations of the usual $SU(3)$ octet and 27 operators while

$$Q_8^s \sim (L_\mu)_{23} \partial^\mu \eta_0 \quad (8)$$

is peculiar to the $U(3)$ framework. Note that the introduction of one extra $\langle \ln U - \ln U^\dagger \rangle \sim \eta_0$ factor in Q_8 , Q_8^m or Q_{27} would violate CPS invariance. Besides, other structures like $(\chi U^\dagger - U \chi^\dagger)_{23} \langle \ln U - \ln U^\dagger \rangle$ can be brought back to Q_8^s through the use of the classical equations of motion. For our purpose, the complete low-energy realization of $\mathcal{H}_{eff}^{\Delta S=1}$ at $\mathcal{O}(p^2)$ is thus given by

$$\mathcal{H}_W^{\Delta S=1} = G_8 Q_8 + G_8^s Q_8^s + G_8^m Q_8^m + G_{27} Q_{27}. \quad (9)$$

Yet the weak mass term Q_8^m is known not to contribute to hadronic observables at leading order, while its higher order effects can be absorbed into a redefinition of the weak counterterms [5, 6]. We will thus disregard it from now. Later, we will check explicitly that the same holds true in respect of radiative kaon decays.

Let us now make a closer connection with the current-current and penguin operators of Eq.(2).

2.2 QCD-inspired alternative basis

As a first step towards an alternative QCD-inspired formulation of Eq.(9), we consider the effective Hamiltonian (1) in the factorization approximation.

In that limit, the chiral realization \hat{Q}_i of the $(V-A) \otimes (V \pm A)$ Q_i operators is straightforward. It simply follows from the hadronization of the left- and right-handed currents in Eq.(7) (with $U \leftrightarrow U^\dagger$ for the right-handed currents). This gives:

$$\begin{aligned} \hat{Q}_1 &= 4 (L_\mu)_{23} (L^\mu)_{11}, & \hat{Q}_2 &= 4 (L_\mu)_{13} (L^\mu)_{21}, \\ \hat{Q}_3 &= -Q_5 = 4 (L_\mu)_{23} \langle L^\mu \rangle, & \hat{Q}_4 &= 4 (L_\mu L^\mu)_{23}. \end{aligned} \quad (10)$$

For the \hat{Q}_6 penguin operator, the situation is more delicate as the constraint $UU^\dagger = 1$ forces us to go beyond Eq.(5) to hadronize the quark densities [7, 8]. From the $\mathcal{O}(p^4)$ strong Lagrangian in the large- N_c limit

$$\mathcal{L}_S^{(p^4, \infty)} \ni \langle \partial_\mu U \partial^\mu U^\dagger (\chi U^\dagger + U \chi^\dagger) \rangle, \langle \chi \square U^\dagger + \square U \chi^\dagger \rangle, \langle (\chi U^\dagger \pm U \chi^\dagger)^2 \rangle, \quad (11)$$

two structures

$$\hat{Q}_6 = 4 (L_\mu L^\mu)_{23} \quad (12)$$

(identical with \hat{Q}_4) and Q_8^m emerge.

Corrections with respect to the factorization approximation consist in meson exchanges between currents or densities. Such $1/N_c$ loop effects, despite formally suppressed, are important due to the quadratic dependence on the physical cut-off for a truncated chiral Lagrangian describing the low-energy strong interactions of massless pseudoscalars in terms of the scale F [9]. Accordingly, no new structure will be induced at $\mathcal{O}(p^2)$ since the other scale parameter m_0 in Eq.(5) has no effect on this fast operator evolution [10]. We thus reach the ansatz:

$$\mathcal{H}_W^{\Delta S=1} = G_W \sum_{i=1}^6 x_i \hat{Q}_i. \quad (13)$$

The overall constant G_W and the weights x_i are not fixed by symmetry arguments. Let us set $G_W \equiv G_F V_{ud} V_{us}^* / \sqrt{2} = 1.77 \times 10^{-12} \text{ MeV}^{-2}$ so that in the factorization approximation (neglecting $V_{td} V_{ts}^*$):

$$x_i \stackrel{FACT.}{=} z_i(\mu_{fact}) \quad (i \neq 6), \quad x_6 \stackrel{FACT.}{=} -r^2 \frac{F_K/F_\pi - 1}{m_K^2 - m_\pi^2} z_6(\mu_{fact}), \quad (14)$$

with μ_{fact} around 1 GeV. The difference $F_K/F_\pi - 1$ is generated by a linear combination of the first two terms of Eq.(11).

The actual x_i values differ from those given in Eq.(14) by long-distance strong interaction effects. Following the principles of chiral expansions, we wish to extract them from phenomenology. Yet only three combinations of x_i are accessible as the corresponding operators can all be expressed in terms of Q_8 , Q_8^s and Q_{27} . Identifying Eqs.(9) and (13), we obtain:

$$\begin{aligned} G_8/G_W &= -\frac{2}{5}x_1 + \frac{3}{5}x_2 + x_4 + x_6 \\ G_8^s/G_W &= \frac{3}{5}x_1 - \frac{2}{5}x_2 + x_3 - x_5 \\ G_{27}/G_W &= \frac{3}{5}(x_1 + x_2). \end{aligned} \quad (15)$$

In order to invert the above system, some extra theoretical assumptions are needed. Corrections with respect to the factorization limit are likely to be important in the case of x_6 due to the presence of the factor $r = 2m_K^2/(m_s + m_d)$ in Eq.(14). We thus have to keep it. However, the situation is different for x_3 , x_4 and x_5 , whose small factorized values suggest marginal effects. Neglecting \hat{Q}_3 , \hat{Q}_4 and \hat{Q}_5 , the QCD-inspired set $(\hat{Q}_1, \hat{Q}_2, \hat{Q}_6)$ becomes equivalent to the basis (Q_8, Q_8^s, Q_{27}) . Notice again that, had we worked in the $SU(3)$ framework, the disappearance of the second octet Q_8^s would have led to a linear relation between \hat{Q}_1 , \hat{Q}_2 and \hat{Q}_6 , rendering thus impossible the distinction between current-current and penguin operators from phenomenology.

2.3 A first look at the weak couplings

Our goal is to extract x_1 , x_2 and x_6 . A first piece of information can readily be obtained from the analysis of the $K \rightarrow \pi\pi$ decays. In the isospin limit ($m_u = m_d$, no electromagnetic corrections), these can be parametrized in terms of two isospin amplitudes, A_0 ($\Delta I = 1/2$) and A_2 ($\Delta I = 3/2$):

$$\begin{aligned} \mathcal{A}(K^0 \rightarrow \pi^+\pi^-) &= A_0 e^{i\delta} + \frac{1}{\sqrt{2}} A_2, \\ \mathcal{A}(K^0 \rightarrow \pi^0\pi^0) &= A_0 e^{i\delta} - \sqrt{2} A_2, \\ \mathcal{A}(K^+ \rightarrow \pi^+\pi^0) &= \frac{3}{2} A_2, \end{aligned} \quad (16)$$

with $\delta \equiv \delta_0 - \delta_2 \simeq \pi/4$, the final state interaction phase shift. In our conventions, A_2 is real and positive in the limit of CP conservation, adopted from now on. The $\Delta I = 1/2$ piece receives contributions from both the Q_8 and Q_{27} operators (none from Q_8^s in the isospin limit), while the $\Delta I = 3/2$ piece is only brought about by Q_{27} . In terms of the x_i 's, this gives:

$$A_0 = \sqrt{2}F \left(G_8 + \frac{1}{9}G_{27} \right) (m_K^2 - m_\pi^2) = \frac{\sqrt{2}}{3}F G_W (-x_1 + 2x_2 + 3x_6) (m_K^2 - m_\pi^2), \quad (17)$$

$$A_2 = \frac{10}{9}F G_{27} (m_K^2 - m_\pi^2) = \frac{2}{3}F G_W (x_1 + x_2) (m_K^2 - m_\pi^2), \quad (18)$$

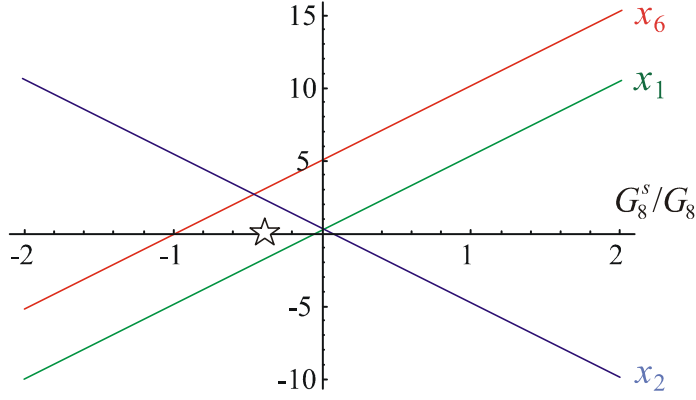


Figure 1: x_1 , x_2 and x_6 as a function of G_8^s/G_8 (G_8 , G_{27} fixed by $K \rightarrow \pi\pi$). The star indicates the QCD-inspired estimate of Eq.(23).

with x_4 neglected (as indicated above) and no contribution from $x_{3,5}$. Experimentally, $\omega^{-1} \equiv A_0/A_2 = 22.2$, which is the very statement of the $\Delta I = 1/2$ rule. This large factor implies a dominance of G_8 over G_{27} :

$$G_8 = 9.1 \times 10^{-12} \text{ MeV}^{-2}, \quad G_{27} = 5.3 \times 10^{-13} \text{ MeV}^{-2}. \quad (19)$$

However, this does not give any information yet on the relative sizes of the x_i 's, and thus on the current-current and penguin fractions in A_0

$$\mathcal{F}_{CC} \equiv \frac{-x_1 + 2x_2}{-x_1 + 2x_2 + 3x_6} \quad \text{and} \quad \mathcal{F}_P \equiv \frac{3x_6}{-x_1 + 2x_2 + 3x_6}. \quad (20)$$

The missing piece of information is of course G_8^s . Before proceeding to its phenomenological determination, let us see what comes out from additional QCD-inspired assumptions. The values of x_1 , x_2 and x_6 corresponding to a given ratio G_8^s/G_8 after imposition of the constraints (19) on the system (15) are depicted in Fig.1. In the case of x_1 and x_2 , strong interaction effects are not expected to change the signs of the factorized values (14), i.e., we should keep $x_1 < 0$ and $x_2 > 0$. This favours a negative ratio G_8^s/G_8 , excluding large positive values of x_6 . A natural scaling further points towards $|G_8^s/G_8| < 1$, which would guarantee $x_i \sim \mathcal{O}(1)$ and also preserve the sign of x_6 with respect to the factorization approximation, i.e., $x_6 > 0$. A small fraction of penguins, as in the factorization approximation at 1 GeV where \mathcal{F}_P is around 20%, would require $x_6 \simeq 1$, i.e., a ratio G_8^s/G_8 as negative as -0.8 . However, another theoretical clue can be obtained from the nonlinear relation between the Wilson coefficients $z_1(\mu)$ and $z_2(\mu)$ derived in the leading logarithmic approximation [1]:

$$(z_2 + z_1)^2 (z_2 - z_1) = 1. \quad (21)$$

Indeed, this relation is known to receive rather small corrections at next-to-leading order (even for μ as low as 700 MeV). Assuming

$$(x_2 + x_1)^2 (x_2 - x_1) = \frac{25G_{27}^2 (G_{27} - 6G_8^s)}{27G_W^3} \simeq 1 \quad (22)$$

to within, say, 30%, would then give the smaller (in absolute value) ratio:

$$(G_8^s/G_8)_{th} = -0.38 \pm 0.12. \quad (23)$$

2.4 Tracking down penguins at the poles

Let us now tackle the phenomenological determination of G_8^s . The vertices induced by Q_8^s always involve one single η_0 field (see Eq.(8)). It is thus natural to turn to η_0 pole contributions to anomaly-driven radiative kaon decays. These proceed through the $\mathcal{O}(p^4)$ Wess-Zumino-Witten (WZW) action of $U(3)$ ChPT, which is for QED external sources [11]:

$$\mathcal{L}_{WZW}^{1\gamma} = \frac{N_c}{48\pi^2} e \varepsilon^{\mu\nu\rho\sigma} A_\mu \langle \partial_\nu U \partial_\rho U^\dagger \partial_\sigma U \{U^\dagger, Q\} \rangle, \quad (24)$$

$$\mathcal{L}_{WZW}^{2\gamma} = \frac{iN_c}{48\pi^2} e^2 \varepsilon^{\mu\nu\rho\sigma} F_{\mu\nu} A_\rho \left(\langle QQ \{ \partial_\sigma U, U^\dagger \} \rangle + \frac{1}{2} \langle QU^\dagger Q \partial_\sigma U - QUQ \partial_\sigma U^\dagger \rangle \right), \quad (25)$$

with A_μ , the electromagnetic field, $F_{\mu\nu} \equiv \partial_\mu A_\nu - \partial_\nu A_\mu$ the corresponding strength tensor, $Q = \text{diag}(Q_u, Q_d, Q_s)$, the light quark charge matrix in units of the positron charge e and $\varepsilon^{\mu\nu\rho\sigma}$, the Levi-Civita tensor with $\varepsilon^{0123} = +1$. Note that in $U(3)$ ChPT, there are additional unnatural parity operators at $\mathcal{O}(p^4)$ (necessarily chiral invariant as unrelated to the WZW action), like for example

$$\varepsilon^{\mu\nu\rho\sigma} F_{\mu\nu} A_\rho \langle QQ \rangle \langle \partial_\sigma U U^\dagger \rangle, \quad (26)$$

but, being $1/N_c$ suppressed, they will be discarded. This is supported by the analysis of the decays $\eta, \eta' \rightarrow \gamma\gamma$, reasonably well reproduced at leading order by Eqs.(25) and (5) alone [12].

In the next sections, we will consider pole-dominated radiative modes like $K_L \rightarrow \gamma\gamma$, $K_S \rightarrow \pi^0\gamma\gamma$ and $K_L \rightarrow \pi^0\pi^0\gamma\gamma$, as well as transitions that receive also other types of contributions like $K^+ \rightarrow \pi^+\gamma\gamma$ and $K_L \rightarrow \pi^+\pi^-\gamma$.

3 The $K_L \rightarrow \gamma\gamma$ decay

Despite a long history, and precise measurements by the NA48 and KLOE Collaborations,

$$\frac{\Gamma(K_L \rightarrow \gamma\gamma)}{\Gamma(K_L \rightarrow \pi^0\pi^0\pi^0)} = \left\{ \begin{array}{l} (2.81 \pm 0.01_{stat} \pm 0.02_{syst}) \times 10^{-3} [13] \\ (2.79 \pm 0.02_{stat} \pm 0.02_{syst}) \times 10^{-3} [14] \end{array} \right\}, \quad (27)$$

it is fair to say that a satisfactory theoretical description of the decay $K_L \rightarrow \gamma\gamma$ is still lacking.

At lowest order in the chiral expansion, i.e. $\mathcal{O}(p^4)$, it proceeds through pseudoscalar poles, as depicted in Fig.2a. In the $SU(3)$ framework, the η_0 is a higher order effect and only the π^0 and η_8 are allowed to propagate, with the result that the amplitude vanishes exactly:

$$\mathcal{A}^{\mu\nu}(K_L \rightarrow \gamma\gamma) \stackrel{SU(3)}{=} \frac{2F\alpha}{\pi} (G_{27} - G_8 + G_8^m) m_K^2 \left(\frac{1}{m_K^2 - m_\pi^2} + \frac{1/3}{m_K^2 - m_{\eta_8}^2} \right) i\varepsilon^{\mu\nu\rho\sigma} k_{1\rho} k_{2\sigma} = 0, \quad (28)$$

upon enforcing the Gell-Mann–Okubo (GMO) mass relation (valid at this order):

$$m_{\eta_8}^2 = \frac{4m_K^2 - m_\pi^2}{3}. \quad (29)$$

The $SU(3)$ decay amplitude therefore starts at $\mathcal{O}(p^6)$, with in particular all the effects of the η_0 . At this stage, phenomenological pole models are constructed [15–19], involving the physical

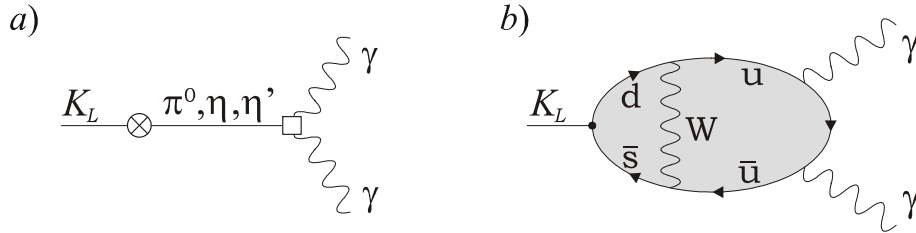


Figure 2: a) Pole diagrams for $K_L \rightarrow \gamma\gamma$. b) Dominant long-distance $\bar{u}u$ contribution.

$\eta^{(\prime)}$ masses but also chiral symmetry breaking parameters for the weak transitions $K_L \rightarrow \pi^0, \eta, \eta'$ and the radiative decays $\pi^0, \eta, \eta' \rightarrow \gamma\gamma$. Yet no definite prediction can be attained because, having a vanishing lowest order, the rate exhibits a high sensitivity to these phenomenological parameters.

3.1 Pole amplitude in U(3) ChPT

In the present work, large- N_c ChPT is used to introduce the effects of the η' state consistently in both the weak and strong Lagrangians Eqs.(5), (9) and (25). The amplitude is then non-vanishing already at $\mathcal{O}(p^4)$, featuring the parameter of interest G_8^s :

$$\mathcal{A}^{\mu\nu}(K_L \rightarrow \gamma\gamma) \stackrel{U(3)}{=} \frac{16F\alpha}{\pi} \left(G_8^s + \frac{2}{3}G_{27} \right) \left(\frac{-m_K^2}{m_0^2 - 3m_K^2 + 3m_\pi^2} \right) i\varepsilon^{\mu\nu\rho\sigma} k_{1\rho} k_{2\sigma}. \quad (30)$$

Yet the contributions of the Q_8 and Q_8^m operators cancel again once the $\eta_8 - \eta_0$ theoretical mass matrix is inserted

$$m_{\eta_8\eta_0}^2 = \begin{pmatrix} \frac{4m_K^2 - m_\pi^2}{3} & \frac{2\sqrt{2}}{3}(m_\pi^2 - m_K^2) \\ \frac{2\sqrt{2}}{3}(m_\pi^2 - m_K^2) & m_0^2 + \frac{2m_K^2 + m_\pi^2}{3} \end{pmatrix}, \quad (31)$$

which corresponds to the generalization of GMO to $U(3)$.

Looking back at Eq.(15), $G_8^s + \frac{2}{3}G_{27}$ is precisely the weight of the \hat{Q}_1 operator. This is the only one able to generate a $\bar{u}u$ pair from the incoming K_L at lowest order ($\hat{Q}_{3,5}$ are again expected to give small contributions, and are discarded). The flavor and color structures of Q_2 prevent \hat{Q}_2 from contributing, while \hat{Q}_6 appears only through its $\bar{d}d + \bar{s}s$ component and cancels out². The decay $K_L \rightarrow \gamma\gamma$ thus proceeds entirely through the long-distance $\bar{s}d(\bar{d}s) \rightarrow \bar{u}u \rightarrow \gamma\gamma$ transition at lowest order (Fig.2b), which is in agreement with a quark-level analysis [16].

Let us stress once more why working in $U(3)$ is essential. Beside the fact that the quark basis $\bar{u}u, \bar{d}d, \bar{s}s$ is ambiguous in $SU(3)$, there are not enough $|\Delta S| = 1$ operators to permit a definite identification of the underlying transitions in this symmetry limit. In fact, \hat{Q}_1, \hat{Q}_2 and \hat{Q}_6 are not independent in $SU(3)$, hence the total $K_L \rightarrow \gamma\gamma$ amplitude has to vanish at $\mathcal{O}(p^4)$ since the last two do not contribute.

The above interpretation can be made obvious by a direct computation in the quark basis:

$$\mathcal{A}^{\mu\nu}(K_L \rightarrow \gamma\gamma) \stackrel{U(3)}{=} V_{weak}^T \cdot P_{LO}(m_K^2) \cdot V_{\gamma\gamma}^{\mu\nu}, \quad (32)$$

²Such a cancellation of the Q_6 penguin operator has already been noticed in the $m_0 \rightarrow 0$ limit [20].

with the LO propagator ($R \equiv 2N_c(m_K^2 - m_\pi^2)/m_0^2$):

$$iP_{LO}(q^2)^{-1} = (q^2 - m_\pi^2) \begin{pmatrix} 1 & 0 & 0 \\ 0 & 1 & 0 \\ 0 & 0 & 1 \end{pmatrix} - \frac{m_0^2}{N_c} \begin{pmatrix} 1 & 1 & 1 \\ 1 & 1 & 1 \\ 1 & 1 & 1+R \end{pmatrix}, \quad (33)$$

the WZW $\gamma\gamma$ vertices (proportional to Q_q^2):

$$V_{\gamma\gamma}^{\mu\nu} = -\frac{\sqrt{2}N_c\alpha}{\pi F} \begin{pmatrix} 4/9 \\ 1/9 \\ 1/9 \end{pmatrix} i\varepsilon^{\mu\nu\rho\sigma} k_{1\rho} k_{2\sigma}, \quad (34)$$

and the weak vertices, in both the (Q_8, Q_8^s, Q_{27}) and $(\hat{Q}_1, \hat{Q}_2, \hat{Q}_6)$ bases (still keeping Q_8^m):

$$V_{weak} = i2\sqrt{2}F^2 m_K^2 \begin{pmatrix} G_8^s + 2G_{27}/3 \\ G_8 - G_8^m + G_8^s - G_{27}/3 \\ G_8 - G_8^m + G_8^s - G_{27}/3 \end{pmatrix} = i2\sqrt{2}F^2 m_K^2 G_W \begin{pmatrix} x_1 \\ x_6 \\ x_6 \end{pmatrix}. \quad (35)$$

The $\bar{d}d$ and $\bar{s}s$ components of V_{weak} are equal due to CPS invariance. One can easily check that only the $\bar{u}u$ component of the weak vector contributes to the amplitude, as announced.

A priori, one could think that NLO effects may reintroduce significant \hat{Q}_6 contributions. This intuition is however based on the pathological $SU(3)$ situation, in which there is an extreme sensitivity due to the inability of $SU(3)$ to catch the leading order $\bar{s}d(\bar{d}s) \rightarrow \bar{u}u \rightarrow \gamma\gamma$ contribution. Once within $U(3)$, this piece is correctly identified and we can consider that NLO effects will behave according to the usual chiral counting, i.e. are at most of 30%. In other words, we will work under the assumption that \hat{Q}_1 represents the dominant contribution to the decay.

3.2 Physical mass prescription

Diagonalizing Eq.(31), the leading order η and η' theoretical (or Lagrangian) masses are found to be

$$m_{\eta(\eta')}^2 = \frac{m_0^2}{2} + m_K^2 \pm \frac{1}{2} \sqrt{m_0^4 - \frac{4}{3}(m_K^2 - m_\pi^2)m_0^2 + 4(m_K^2 - m_\pi^2)^2}. \quad (36)$$

The parameter m_0 has to be fitted to reproduce both m_η and $m_{\eta'}$ as close as possible to their physical values, which gives m_0 between 800 and 900 MeV. From Fig.3, the masses are then well reproduced, within less than 15%, which is quite consistent with chiral counting for higher order effects.

Still, in the present work, we are mainly concerned by pole amplitudes, i.e. amplitudes involving virtual $\eta - \eta'$ exchanges. For such processes, a good physical mass prescription must ensure correct analytical properties, i.e., freeze the poles at their right places. Varying m_0 is therefore not satisfactory. In analogy with the usual $\mathcal{O}(p^2)$ substitutions

$$\begin{aligned} m_\pi^2 &= \frac{r}{2} (m_u + m_d) \rightarrow M_\pi^2 \simeq (135 \text{ MeV})^2, \\ m_K^2 &= \frac{r}{2} (m_s + m_{u,d}) \rightarrow M_K^2 \simeq (495 \text{ MeV})^2, \end{aligned} \quad (37)$$

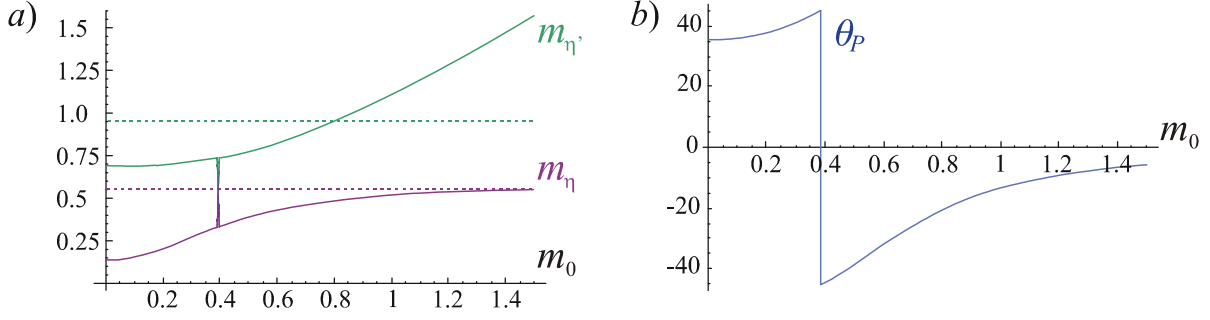


Figure 3: $\eta - \eta'$ masses (in GeV) and mixing angle at lowest order in large- N_c $U(3)$ ChPT.

our prescription is to substitute for the LO mass matrix Eq.(31) the most general mass matrix compatible with isospin symmetry³. In the $\bar{u}u, \bar{d}d, \bar{s}s$ basis considered in Eq.(33), the (π^0, η_8, η_0) propagator takes then the generic form

$$iP_{phys}(q^2)_{\bar{q}q}^{-1} = (q^2 - M_\pi^2) \begin{pmatrix} 1 & 0 & 0 \\ 0 & 1 & 0 \\ 0 & 0 & 1 \end{pmatrix} - \frac{M_0^2}{3} \begin{pmatrix} 1 & 1 & 1 - \delta \\ 1 & 1 & 1 - \delta \\ 1 - \delta & 1 - \delta & 1 + \bar{R} - 2\delta \end{pmatrix}, \quad (38)$$

with M_0, δ, \bar{R} , some parameters to be adjusted to freeze the poles at their physical values. Equivalently, working in the η_8, η_0 basis, this propagator can be written

$$iP_{phys}(q^2)_{\eta_8\eta_0}^{-1} = \begin{pmatrix} \cos \theta_P & \sin \theta_P \\ -\sin \theta_P & \cos \theta_P \end{pmatrix} \begin{pmatrix} q^2 - M_\eta^2 & 0 \\ 0 & q^2 - M_{\eta'}^2 \end{pmatrix} \begin{pmatrix} \cos \theta_P & -\sin \theta_P \\ \sin \theta_P & \cos \theta_P \end{pmatrix}, \quad (39)$$

and the π^0 does not mix (for the model-independent relationship between Eqs.(38) and (39), see Ref. [21]). The masses are then fixed to

$$M_\eta \simeq 547.8 \text{ MeV}, \quad M_{\eta'} \simeq 957.8 \text{ MeV}, \quad (40)$$

with the mixing angle around $\theta_P \simeq -22^\circ$ if a large- N_c limit is taken at each order in the momentum expansion [21].

When the leading order is non-zero, inserting physical masses amounts to including a particular class of higher order effects. Yet there are still many other sources of corrections, and to get a handle on their order of magnitude, we will consider θ_P as an effective angle, allowed to vary around -22° . Specifically, the sensitivity of the pole amplitudes will be probed by taking θ_P inside the range $[-15^\circ, -25^\circ]$.

For example, we could include, in addition to the mass corrections, the deviations from $F_\eta = F_{\eta'} = F_\pi$ by introducing the renormalized decay constant matrix \mathbf{F}_η as

$$P_{phys}(q^2)'_{\eta_8\eta_0} = F^2 (\mathbf{F}_\eta)^{-1} \cdot (P_{phys}(q^2)_{\eta_8\eta_0}) \cdot (\mathbf{F}_\eta^T)^{-1}. \quad (41)$$

This amounts to switching to a two-mixing angle formalism since by definition

$$\begin{pmatrix} \cos \theta_P & -\sin \theta_P \\ \sin \theta_P & \cos \theta_P \end{pmatrix} \mathbf{F}_\eta \equiv \begin{pmatrix} F_8^\eta & F_0^\eta \\ F_8^{\eta'} & F_0^{\eta'} \end{pmatrix} \equiv \begin{pmatrix} F_8 \cos \theta_8 & -F_0 \sin \theta_0 \\ F_8 \sin \theta_8 & F_0 \cos \theta_0 \end{pmatrix}. \quad (42)$$

³In principle, the pseudoscalar widths have to be included to really ensure correct analytical properties. However, these are numerically not relevant and will be neglected.

However, not much is gained by using this prescription instead of Eq.(39) as there are still unaccounted NLO effects beyond masses and decay constants. Numerically, we have checked that in all the cases considered, taking Eq.(42) with the values of F_8 , F_0 , θ_8 and θ_0 from either the large N_c analysis of Ref. [12] or the phenomenological fit of Ref. [22] does not alter our conclusions (in general, the deviation with respect to Eq.(39) with $\theta_P \simeq -22^\circ$ can be accounted for by taking $\theta_P \simeq -15^\circ$ or slightly smaller).

3.3 The $K_L \rightarrow \gamma\gamma$ rate and its implications for the $\Delta I = 1/2$ rule

Naively enforcing the physical mass prescription, i.e. taking Eq.(32) with the propagator Eq.(38), would however reintroduce a large \hat{Q}_6 contribution. This is a spurious effect because it corresponds to the partial inclusion of higher order terms (only those from mass corrections) for a contribution which vanishes at lowest order. As said before, the decay should be dominated by the $\bar{u}u$ transition, hence large cancellations are expected to occur for \hat{Q}_6 at NLO (indications of these are discussed in the next subsection).

On the contrary, since the $\bar{u}u$ part is non-vanishing at lowest order, inserting the physical masses instead of the Lagrangian ones is allowed. Therefore, we definitively discard the $\bar{d}d$ and $\bar{s}s$ components from the weak vertex:

$$V_{weak} = i2\sqrt{2}F^2m_K^2G_W \begin{pmatrix} x_1 \\ 0 \\ 0 \end{pmatrix} = i2\sqrt{2}F^2m_K^2 \begin{pmatrix} G_8^s + \frac{2}{3}G_{27} \\ 0 \\ 0 \end{pmatrix}, \quad (43)$$

and use Eq.(38) to reach the final form for the amplitude ($c_\theta \equiv \cos\theta_P$, $s_\theta \equiv \sin\theta_P$):

$$\begin{aligned} \mathcal{A}^{\mu\nu}(K_L \rightarrow \gamma\gamma) &= \frac{2F\alpha}{\pi} \left(G_8^s + \frac{2}{3}G_{27} \right) M_K^2 i\varepsilon^{\mu\nu\rho\sigma} k_{1\rho} k_{2\sigma} \\ &\times \left(\frac{1}{M_K^2 - M_\pi^2} + \frac{(c_\theta - 2\sqrt{2}s_\theta)(c_\theta - \sqrt{2}s_\theta)}{3(M_K^2 - M_\eta^2)} + \frac{(s_\theta + 2\sqrt{2}c_\theta)(s_\theta + \sqrt{2}c_\theta)}{3(M_K^2 - M_{\eta'}^2)} \right). \end{aligned} \quad (44)$$

Numerically, this amplitude is dominated by the η pole:

$$\mathcal{A}^{\mu\nu}(K_L \rightarrow \gamma\gamma) = \left(G_8^s + \frac{2}{3}G_{27} \right) \left[(0.46)_\pi - (1.83 \pm 0.30)_\eta - (0.12 \pm 0.02)_{\eta'} \right] i\varepsilon^{\mu\nu\rho\sigma} k_{1\rho} k_{2\sigma}, \quad (45)$$

where the numbers are in MeV and the errors amount to varying θ_P between -15° and -25° . The parametrization is rather stable with respect to $\eta - \eta'$ mixing parameters, which means that the amplitude is under control once the poles are frozen at their right places. Then, from the experimental values Eqs.(27) with $\Gamma(K_L \rightarrow \pi^0\pi^0\pi^0)$ from [23, 24], the only free parameter can be extracted up to a two-fold ambiguity:

$$(G_8^s/G_8)_{ph} \simeq \pm 1/3. \quad (46)$$

From QCD-inspired arguments, the positive solution is discarded as it would lead to x_1, x_2 of the wrong signs and x_6 very large (see Fig.1). The negative solution

$$(G_8^s/G_8)_{ph+th} = -0.30 \pm 0.05 \quad (47)$$

is detailed in Table 1 and Fig.4. Also, $(x_1 + x_2)^2(x_2 - x_1)$ stays remarkably close to one, which means that the low energy evolution of current \times current operators is indeed rather smooth.

$\theta_P(^{\circ})$	G_8^s/G_8	x_1	x_2	x_6	$(x_1 + x_2)^2(x_2 - x_1)$	$\mathcal{F}_{CC}(\%)$	$\mathcal{F}_P(\%)$
-10	-0.44	-2.06	2.56	2.78	1.15	46	54
-15	-0.35	-1.59	2.08	3.26	0.91	37	63
-17.5	-0.32	-1.42	1.92	3.42	0.83	34	66
-20	-0.29	-1.29	1.78	3.56	0.76	31	69
-22.5	-0.27	-1.18	1.67	3.67	0.71	29	71
-25	-0.25	-1.08	1.58	3.76	0.66	27	73
-30	-0.22	-0.94	1.44	3.90	0.59	25	75

Table 1: The coupling G_8^s as extracted from $K_L \rightarrow \gamma\gamma$, in terms of θ_P , and the corresponding weights x_i for the current \times current and penguin operators. The last two columns give the current \times current and penguin fractions in A_0 defined in Eq.(20).

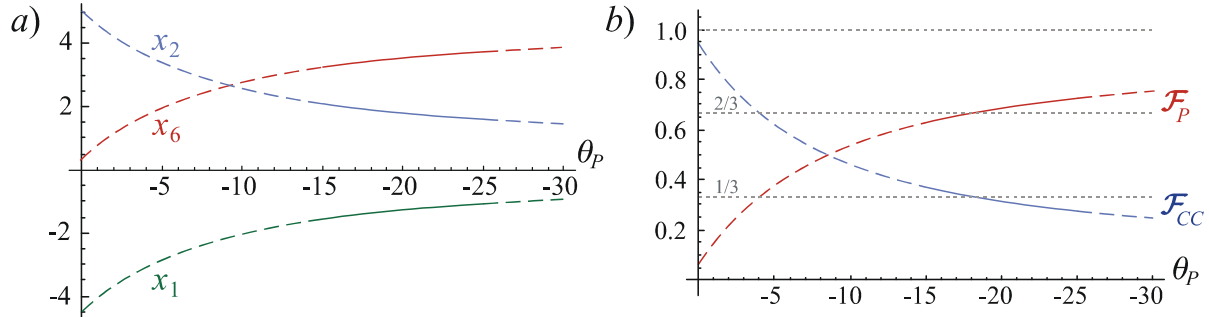


Figure 4: Graphical representation of Table 1: a) Weak operator weights x_i as a function of θ_P , b) Corresponding current \times current and penguin fractions in A_0 .

On the other hand, x_6 increases quite dramatically from its perturbative QCD value Eq.(14) and appears responsible for about 2/3 of the $\Delta I = 1/2$ enhancement

$$\mathcal{F}_P = (68 \pm 6) \% \quad (48)$$

where the error reflects only the variation of θ_P . Let us stress again that x_1 , x_2 and x_6 are the weights of the weak operators at a very low hadronic scale, around the ChPT scale F . It is intuitively clear then that x_6 , and thus \mathcal{F}_P , can be large since we allow the evolution $Q_1, Q_2 \rightarrow Q_6$ all the way down to this scale.

3.4 Effective suppression of Q_6 at higher order

In the context of $SU(3)$, there is only one weak octet operator, hence it is clear that large $\mathcal{O}(p^6)$ “ Q_8 ” effects are present. Indeed, it is through the counterterms that the leading $\bar{s}d(\bar{d}s) \rightarrow \bar{u}u \rightarrow \gamma\gamma$ transition is reconstructed. Yet, this reconstruction is not trivial and implies a specific interplay between strong and weak counterterms of both $\mathcal{O}(p^4)$ and $\mathcal{O}(p^6)$, corresponding to corrections to the decay constants, two-photon vertices, masses (i.e., corrections to GMO) and weak transitions.

In the appendix, the complete analysis of $K_L \rightarrow \gamma\gamma$ at $\mathcal{O}(p^6)$ in $SU(3)$ ChPT is presented. It is shown that, to a large extent, the counterterms either act together to reconstruct \hat{Q}_1 , or cancel among themselves. For example, corrections brought by $F_{\eta 8} \neq F_\pi$ cancel out with some

mass corrections, and are thus at least of $\mathcal{O}(p^8)$. Only a small irreducible combination of (scalar-saturated) counterterms survives, on which not much can be said at present. Still, given the dynamical insight gained, it is reasonable to expect this combination to be small. In conclusion, there is a clear indication that no large contribution from \hat{Q}_6 is generated at $\mathcal{O}(p^6)$ in $SU(3)$ ChPT.

Something very similar should happen in $U(3)$, but it is unfortunately difficult to be as quantitative since we do not have any handle on the $U(3)$ weak counterterms. Anyway, here also, it is likely that corrections to the masses, decay constants, weak and WZW vertices cancel among themselves, at least in part, for the \hat{Q}_6 contribution.

This is to be contrasted to the phenomenological pole model analyses [17,18], which overlook cancellations among $\mathcal{O}(p^6)$ corrections. To be more specific, these models usually introduce a parameter ρ to account for nonet symmetry breaking. In $U(3)$, this breaking is entirely due to the Q_8^s and Q_{27} operators (which induce only $K_L \rightarrow \eta_0$ and $K_L \rightarrow \pi^0, \eta_8$ transitions, respectively):

$$\rho - 1 \equiv -\frac{1}{2} \sqrt{\frac{3}{2}} \frac{\langle \eta_0 | \mathcal{H}_W^{\Delta S=1} | K_L \rangle}{\langle \pi^0 | \mathcal{H}_W^{\Delta S=1} | K_L \rangle} - 1 = \frac{3 G_8^s + 2G_{27}/3}{2 G_8 - G_{27}} = \frac{3}{2} \frac{x_1}{x_6 - x_1}. \quad (49)$$

Obviously, the nonet symmetry limit, $\rho = 1$, amounts to discarding the dominant \hat{Q}_1 contribution (i.e. $K_L \rightarrow \bar{u}u \rightarrow \gamma\gamma$), and keeping only the \hat{Q}_6 one. Therefore, in that limit, these models should under-estimate the $K_L \rightarrow \gamma\gamma$ rate, but this is not the case (on the contrary, they need $\rho < 1$ to *reduce* the \hat{Q}_6 contribution). In other words, from the dominance of the $K_L \rightarrow \bar{u}u \rightarrow \gamma\gamma$ transition, a correct phenomenological pole model should be proportional to $\rho - 1$ (like Eq.(44)), to a good approximation.

3.5 Comments on $K_L \rightarrow \gamma\gamma^*$

For the $K_L \rightarrow \gamma\ell^+\ell^-$ decays, a detailed slope analysis was performed in Ref. [25], including vector meson exchanges. Two remarks can be made from the insight gained here.

First, quite generally, our two-step phenomenological procedure to deal with pole amplitudes in $U(3)$ could have some implications also for VMD-type models. Indeed, working first with theoretical masses permits the identification of vanishing contributions, for which it is very dangerous to include only partially the higher order corrections (due only to the masses for example). As a rule, cancellations plague pole amplitudes and should be dealt with carefully. This is especially true in $SU(3)$ ChPT, since it is unable to catch a transition through a $\bar{u}u$ quark pair at leading order. Only once the surviving terms are precisely identified, one is allowed to switch to physical masses without risks.

Given the specific topologies studied in Ref. [25], it is the parameter b_V^{nonet} that could appear most sensitive to the previous remark. It originates from the processes $K_L \rightarrow \pi^0, \eta, \eta' \rightarrow \gamma(\rho, \omega, \phi) \rightarrow \gamma\gamma^*$, which vanish at lowest order in $SU(3)$ ChPT, and proceed through $G_8^s + \frac{2}{3}G_{27}$ in $U(3)$ ChPT. However, all the dependences on the weak transition cancel in the normalization with respect to $K_L \rightarrow \gamma\gamma$, and b_V^{nonet} as given in Ref. [25] is not modified.

Second, it is to be noted that the global sign of our $K_L \rightarrow \gamma\gamma$ amplitude when $G_8^s/G_8 < 0$ is opposite to the one obtained using phenomenological pole models⁴. This is supported by the analysis of Ref. [25]. Yet, a precise constraint on G_8^s/G_8 from $K_L \rightarrow \gamma\gamma^*$ seems at present

⁴These models in general imply a destructive interference between the η and η' poles, leaving the π^0 one as dominant (see the discussion in [18]). Then, one can see (independently of our conventions) that the sign of the π^0 pole in Eq.(28), keeping only G_8 , is the opposite of the η one of Eq.(45) when $G_8^s/G_8 < 0$.

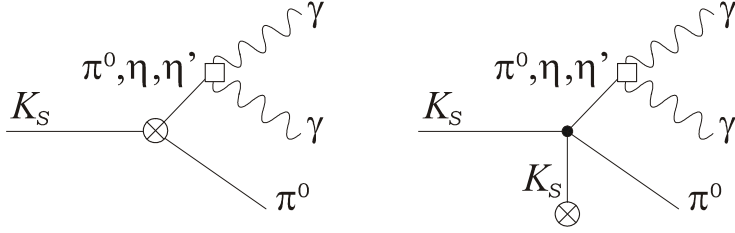


Figure 5: Pole and tadpole diagrams for the process $K_S \rightarrow \pi^0 \gamma \gamma$.

difficult to obtain given the many unknown counterterms and VMD couplings. So, the purpose of the remaining sections is to search for independent constraints on G_8^s/G_8 from other radiative K decays.

4 The $K_S \rightarrow \pi^0 \gamma \gamma$ decay

The radiative process $K_S \rightarrow \pi^0 \gamma \gamma$ is the simplest mode one can think of to test the physical mechanism advocated for $K_L \rightarrow \gamma \gamma$, with in particular $G_8^s/G_8 \simeq -1/3$. The corresponding branching fraction has been measured two years ago by the NA48 collaboration, though with large uncertainties [26]:

$$\mathcal{B}(K_S \rightarrow \pi^0 \gamma \gamma)_{m_{\gamma\gamma} > 220 \text{ MeV}}^{\text{exp}} = (4.9 \pm 1.8) \times 10^{-8} . \quad (50)$$

The decay proceeds through pole diagrams at leading order [27], with also a tadpole graph in the case of the weak mass operator Q_8^m [28] (Fig.5). Unlike for $K_L \rightarrow \gamma \gamma$, the amplitude starts at $\mathcal{O}(p^4)$ in both $U(3)$ and $SU(3)$ ChPT. It can be parametrized in terms of a pole function $B(T^2)$:

$$\mathcal{A}^{\mu\nu}(K_S \rightarrow \pi^0 \gamma \gamma) = \frac{8\alpha}{3\pi} B(T^2) \varepsilon^{\mu\nu\rho\sigma} k_{1\rho} k_{2\sigma} , \quad (51)$$

with $T = k_1 + k_2$, the total momentum of the photon pair. This gives for the width:

$$\Gamma(K_S \rightarrow \pi^0 \gamma \gamma) = \frac{2\alpha^2 M_K^5}{9(2\pi)^5} \int_{0.2}^{z_{\text{max}}} dz \lambda^{1/2}(1, z, r_\pi^2) z^2 |B(z)|^2 , \quad (52)$$

with $z = T^2/M_K^2$, $\lambda(a, b, c) = a^2 + b^2 + c^2 - 2ab - 2ac - 2bc$, $r_\pi = M_\pi/M_K$ and $z_{\text{max}} = (1 - r_\pi)^2 \simeq 0.53$. The infrared cut-off is introduced to get rid of the $K_S \rightarrow \pi^0 \pi^0$ background as in Eq.(50).

4.1 Pole amplitude in $U(3)$ ChPT

A tree-level $U(3)$ computation gives:

$$B(T^2) = (m_K^2 - m_\pi^2) [G_8 B_8(T^2) + G_8^s B_8^s(T^2) + G_{27} B_{27}(T^2)] \quad (53)$$

with no contribution from Q_8^m and

$$\begin{aligned} B_8(T^2) &= \frac{(m_K^2 - T^2)(m_0^2 - m_\pi^2 + T^2)}{(T^2 - m_\eta^2)(T^2 - m_{\eta'}^2)(T^2 - m_\pi^2)} , & B_8^s(T^2) &= \frac{5m_K^2 - 2m_\pi^2 - 3T^2}{2(T^2 - m_\eta^2)(T^2 - m_{\eta'}^2)} , \\ B_{27}(T^2) &= \frac{3m_0^2(T^2 - m_K^2) + 2(m_K^2 - m_\pi^2)(T^2 - m_\pi^2)}{3(T^2 - m_\eta^2)(T^2 - m_{\eta'}^2)(T^2 - m_\pi^2)} . \end{aligned} \quad (54)$$

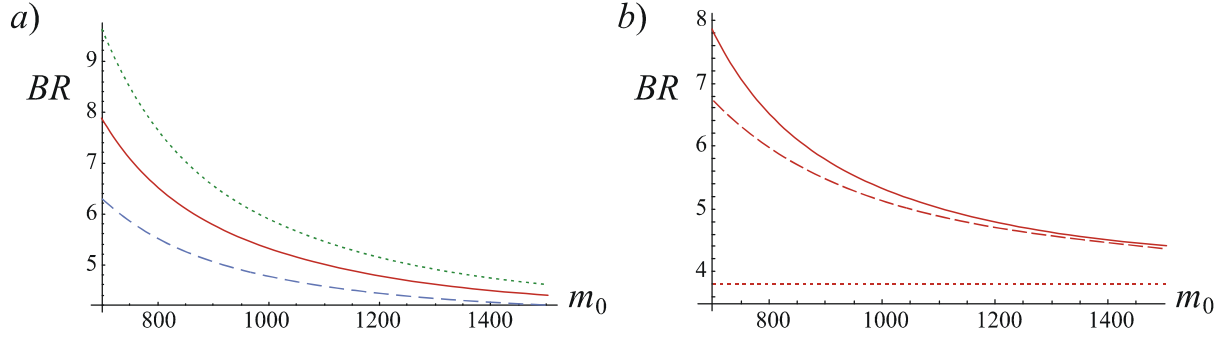


Figure 6: a) $\mathcal{B}(K_S \rightarrow \pi^0 \gamma \gamma)$, $\times 10^8$, as a function of m_0 for $G_8^s/G_8 = -0.3, 0, +0.3$ (dashed, plain, dotted). b) Comparison between the $\mathcal{O}(p^4)$ $SU(3)$ result (dotted), idem plus the m_0^{-2} corrections (dashed), and full $\mathcal{O}(p^4)$ $U(3)$ result (plain), with $G_8^s = 0$ for the three curves.

Note that $m_{\pi, K, \eta, \eta'}$ refer to the *theoretical* masses, defined in Eqs.(36) and (37). It is only when these masses are used (i.e., when one works consistently at lowest order) that the weak mass term Q_8^m indeed drops out. Note also the identity

$$\frac{3}{5}B_8 - \frac{2}{5}B_8^s + \frac{3}{5}B_{27} = 0, \quad (55)$$

originating from the fact that \hat{Q}_2 cannot contribute to any of the subprocesses $K_S \rightarrow \pi^0(\pi^0, \eta, \eta')$.

The behavior of the rate as a function of m_0 is plotted in Fig.6a. A significant enhancement is observed when m_0 decreases. This is essentially an effect of the η pole, that comes closer to the upper boundary of phase-space when m_0 diminishes (Fig.3a). In fact, this pole could even enter the phase-space if m_0 was chosen as low as $m_0 < 447$ MeV, which corresponds to $m_\eta < m_K - m_\pi$ from Eq.(36). Such a value is of course to be avoided. The estimation of the actual enhancement requires the phenomenological prescription proposed in Sec.3.2, and is deferred to Sec.4.3.

On the other hand, it is clear that, Q_8 being allowed to contribute at leading order, it will dominate the decay via the pion pole (and, to a lesser extent, the η one). This explains the moderate sensitivity of $\mathcal{B}(K_S \rightarrow \pi^0 \gamma \gamma)$ to G_8^s exhibited in Fig.6a. However, the decay $K_S \rightarrow \pi^0 \gamma \gamma$ could still be a useful probe of G_8^s/G_8 , as will be discussed in Sec.4.3.

4.2 Reduction to $SU(3)$ ChPT

How can the predicted enhancement for decreasing m_0 (see Fig.6a) be understood from the point of view of the $SU(3)$ chiral expansion? In order to answer that question, let us develop the three pole functions (54) in powers of $1/m_0^2$:

$$\begin{aligned} B_8(T^2) &= \frac{T^2 - m_K^2}{(T^2 - m_{\eta_8}^2)(T^2 - m_\pi^2)} - \frac{2(5m_K^2 - 2m_\pi^2 - 3T^2)(T^2 - m_K^2)}{3(T^2 - m_{\eta_8}^2)^2 m_0^2} + \mathcal{O}(m_0^{-4}), \\ B_8^s(T^2) &= 0 - \frac{5m_K^2 - 2m_\pi^2 - 3T^2}{2(T^2 - m_{\eta_8}^2)m_0^2} + \mathcal{O}(m_0^{-4}), \\ B_{27}(T^2) &= -\frac{T^2 - m_K^2}{(T^2 - m_{\eta_8}^2)(T^2 - m_\pi^2)} - \frac{(5m_K^2 - 2m_\pi^2 - 3T^2)(2m_K^2 + m_\pi^2 - 3T^2)}{9(T^2 - m_{\eta_8}^2)^2 m_0^2} + \mathcal{O}(m_0^{-4}), \end{aligned} \quad (56)$$

with $m_{\eta_8}^2$ fixed by the GMO relation. Though Eq.(54) is just the $\mathcal{O}(p^4)$ $U(3)$ amplitude, the various terms in the above series correspond to increasing p^2 orders in $SU(3)$. As can be checked numerically, these series are quite well-behaved (i.e., as expected from naive chiral counting). Still, significant effects can build up through phase-space integration, leading to the large enhancement observed in Fig.6a. The behavior of the total rate as a function of m_0 when the m_0 series is truncated at a given order is displayed in Fig.6b:

- Retaining only the $\mathcal{O}(m_0^0)$ terms, the $\mathcal{O}(p^4)$ $SU(3)$ result [27] is recovered (dotted line in Fig.6b):

$$\mathcal{B}(K_S \rightarrow \pi^0 \gamma \gamma)_{z>0.2}^{SU(3), \mathcal{O}(p^4)} = 3.8 \times 10^{-8}. \quad (57)$$

- Terms of order m_0^{-2} introduce a class of $\mathcal{O}(p^6)$ effects, leading in $1/N_c$, which corresponds exactly to the $L_7, N_{13}, L_9^{(6)}$ and $N_1^{(6)}$ counterterms once these are saturated by η_0 exchanges (see appendix, Eqs.(96,97,100)). They are seen to conspire collectively at the rate level (dashed line in Fig.6b), already without G_8^s , in order to reproduce the effect of the η pole as a function of m_0 discussed before.
- Keeping the full $U(3)$ result comes to keeping some leading $1/N_c$ contributions at all orders. As the plain line in Fig.6b shows, the leading $1/N_c$ terms of order $\mathcal{O}(p^{n>6})$ amount to only a small correction to the rate (at least as long as m_0 is not too small).

4.3 The $K_S \rightarrow \pi^0 \gamma \gamma$ rate and its sensitivity to the penguin fraction

One of the advantages of dealing with η_0 effects in the $U(3)$ framework rather than through $SU(3)$ local counterterms is that we do not have to face the problem of fixing the m_0 parameter. Indeed, as discussed in Sec.3.2, the requirement of freezing the pseudoscalar poles at their right places, thereby restoring the analytical properties of the amplitude, leads to a well-defined prescription. Since both \hat{Q}_1 and \hat{Q}_6 contribute at lowest order, Eq.(39) can be used directly, and we get to

$$\begin{aligned} B_8(T^2) &= \frac{3(2M_K^2 - M_\pi^2 - T^2)}{8(M_K^2 - M_\pi^2)(T^2 - M_\pi^2)} - \frac{2M_K^2 + M_\pi^2 - 3T^2}{8(M_K^2 - M_\pi^2)} \left(\frac{c_\theta c_\eta}{T^2 - M_\eta^2} + \frac{s_\theta c_{\eta'}}{T^2 - M_{\eta'}^2} \right) \\ &\quad + \frac{1}{2\sqrt{2}} \left(\frac{s_\theta c_\eta}{T^2 - M_\eta^2} - \frac{c_\theta c_{\eta'}}{T^2 - M_{\eta'}^2} \right), \quad (58) \\ B_8^s(T^2) &= \frac{3}{4\sqrt{2}} \left(\frac{s_\theta c_\eta}{T^2 - M_\eta^2} - \frac{c_\theta c_{\eta'}}{T^2 - M_{\eta'}^2} \right), \\ B_{27}(T^2) &= \frac{-3(2M_K^2 - M_\pi^2 - T^2)}{8(M_K^2 - M_\pi^2)(T^2 - M_\pi^2)} + \frac{2M_K^2 + M_\pi^2 - 3T^2}{8(M_K^2 - M_\pi^2)} \left(\frac{c_\theta c_\eta}{T^2 - M_\eta^2} + \frac{s_\theta c_{\eta'}}{T^2 - M_{\eta'}^2} \right), \end{aligned}$$

with $c_\eta \equiv c_\theta - 2\sqrt{2}s_\theta$ and $c_{\eta'} \equiv s_\theta + 2\sqrt{2}c_\theta$, the mixing angle combinations for η and $\eta' \rightarrow \gamma\gamma$, respectively (as a consistency check, note that Eq.(55) is preserved).

The resulting differential rate for $z > 0.2$ is shown in Fig.7a. Yet its shape is not much affected by neither θ_P nor G_8^s/G_8 , and extracting information on the latter is clearly beyond foreseeable experimental sensitivity. Looking at the low-energy end of the $\gamma\gamma$ spectrum would not be more helpful. Indeed, integrating over $0 < z < 0.048$ ($m_{\gamma\gamma} < 108$ MeV), the obtained

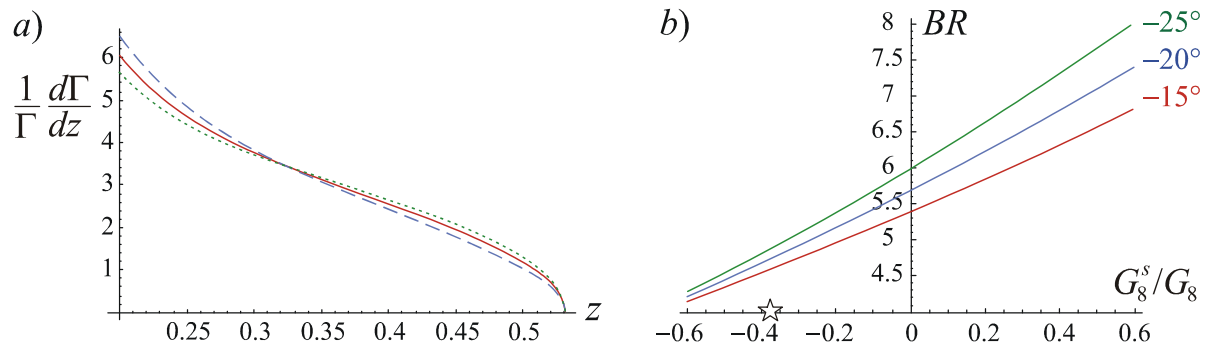


Figure 7: a) $K_S \rightarrow \pi^0 \gamma \gamma$ normalized differential rate for $\theta_P = -20^\circ$, $G_8^s/G_8 = -0.3, 0, +0.3$ (dashed, plain, dotted). b) $\mathcal{B}(K_S \rightarrow \pi^0 \gamma \gamma)$, $\times 10^8$, as a function of G_8^s/G_8 for $\theta_P = -15^\circ, -20^\circ, -25^\circ$. The star refers to Eq.(23).

partial branching ratio varies from 0.48×10^{-8} to 0.44×10^{-8} for G_8^s/G_8 between -0.6 and 0.6 , while the $SU(3)$ prediction is 0.49×10^{-8} .

Fortunately, for the total rate, the situation is better though, as said before, G_8^s is not dominant. Fig.7b summarizes the constraints one could get on G_8^s/G_8 from an experimental determination of the branching ratio. Note that merely fixing the sign of G_8^s/G_8 (inaccessible from $K_L \rightarrow \gamma \gamma$ alone) would already give valuable information on the low-energy realization of the effective weak Hamiltonian (1).

Of course, Fig.7b is subject to the theoretical uncertainties associated with any leading order ChPT computation. A precise extraction of G_8^s/G_8 from $K_S \rightarrow \pi^0 \gamma \gamma$ would require an estimation of the NLO effects. While some unitary corrections are already included through the use of G_8 as extracted from $K_S \rightarrow \pi \pi$, there remains the separate class of $\mathcal{O}(p^6)$ effects from vector mesons. These were seen to give sizeable contributions to $K_L \rightarrow \pi^0 \gamma \gamma$ (see Ref. [29] for a recent review and list of references) and though the underlying dynamics is very different for $K_S \rightarrow \pi^0 \gamma \gamma$, working out their impact would be really called for. In particular, one should investigate if they affect either the differential rate (Fig.7a) or the total rate for low $\gamma \gamma$ invariant mass, which are pretty much insensitive to G_8^s/G_8 and θ_P . In that case, these two observables would provide essential discriminating tools, able to single out the $\mathcal{O}(p^6)$ corrections due to vector resonances.

Finally, one can predict $\mathcal{B}(K_S \rightarrow \pi^0 \gamma \gamma)$ from the range of G_8^s/G_8 preferred by Eq.(22) (which englobes the one extracted from $K_L \rightarrow \gamma \gamma$, see Eq.(47)):

$$G_8^s/G_8 = -0.38 \pm 0.12 \Rightarrow \mathcal{B}(K_S \rightarrow \pi^0 \gamma \gamma)_{z>0.2}^{U(3), \mathcal{O}(p^4)} = (4.8 \pm 0.5) \times 10^{-8}, \quad (59)$$

where the error, inferred from Fig.7b, includes the theoretical uncertainties associated with the physical mass prescription (i.e., with a class of $\mathcal{O}(p^6)$ effects). As expected, the effect of the η_0 meson increases the $\mathcal{O}(p^4)$ $SU(3)$ prediction (57). Note that both results are in agreement with the (still imprecise) experimental value (50).

5 The $K^+ \rightarrow \pi^+ \gamma \gamma$ decay

Let us now turn to $K^+ \rightarrow \pi^+ \gamma \gamma$, which has already received a lot of attention. Experimentally, the situation has been improved recently [30] and is expected to get even better in the near

future. On the theoretical side, the analysis is slightly more involved than for $K_S \rightarrow \pi^0 \gamma \gamma$ as there are now both loop and pole contributions at $\mathcal{O}(p^4)$ [31]:

$$\mathcal{A}^{\mu\nu} (K^+ \rightarrow \pi^+ \gamma \gamma) = \frac{\alpha}{4\pi} \left[A(T^2) (T^2 g^{\mu\nu} - 2k_1^\nu k_2^\mu) + B(T^2) \varepsilon^{\mu\nu\rho\sigma} k_{1\rho} k_{2\sigma} \right], \quad (60)$$

with $A(T^2)$, the π^\pm, K^\pm loop function, and $B(T^2)$, the π^0, η, η' pole one. These two pieces do not interfere in the rate since they produce the two photons in different CP states:

$$\Gamma (K^+ \rightarrow \pi^+ \gamma \gamma) = \frac{\alpha^2 M_K^5}{16(4\pi)^5} \int_{0.2}^{z_{\max}} dz \lambda^{1/2} (1, z, r_\pi^2) z^2 \left[4|A(z)|^2 + |B(z)|^2 \right], \quad (61)$$

where the cut in z is applied to remove the $K^+ \rightarrow \pi^+ \pi^0$ background. Though the loop contribution is larger than the pole one, this latter piece should not be neglected. Indeed, as we will see, it is very sensitive to the ratio G_8^s/G_8 thanks to the suppression of the π^0 pole compared to the η, η' ones ($K^+ \rightarrow \pi^+ \pi^0$ is a $\Delta I = 3/2$ transition).

5.1 Loop amplitude in SU(3) ChPT

For the $A(z)$ amplitude, working with the enlarged symmetry $U(3)$ would be superfluous as only charged particles circulate the loop. We will thus take up the standard $\mathcal{O}(p^4)$ $SU(3)$ result [31]:

$$A(z) = G_8 \left[\left(1 + \frac{1}{z} - \frac{r_\pi^2}{z} + \delta_{27}^\pi \right) \Phi(z/r_\pi^2) + \left(1 - \frac{1}{z} + \frac{r_\pi^2}{z} + \delta_{27}^K \right) \Phi(z) - \hat{c} \right],$$

$$\delta_{27}^\pi = \frac{G_{27}}{G_8} \left(\frac{13r_\pi^2}{3z} + \frac{7}{3z} - \frac{13}{3} \right), \quad \delta_{27}^K = \frac{G_{27}}{G_8} \left(\frac{7r_\pi^2}{3z} + \frac{13}{3z} - \frac{13}{3} \right), \quad (62)$$

with the three-point loop functions

$$\Phi(a) = \begin{cases} 1 - \frac{4}{a} \arcsin^2 \sqrt{a/4} & 4/a > 1 \\ 1 + \frac{1}{a} \left(\log \frac{1 - \sqrt{1-4/a}}{1 + \sqrt{1-4/a}} + i\pi \right)^2 & 0 < 4/a < 1. \end{cases} \quad (63)$$

The contributions of the counterterms are collected in the unknown constant \hat{c} :

$$\hat{c} = \frac{128\pi^2}{3} \left(3(L_9 + L_{10}) + N_{14} - N_{15} - 2N_{18} + \frac{2G_{27}}{3G_8} (3(L_9 + L_{10}) + D_i) \right), \quad (64)$$

where the L_i 's refer to the basis of $\mathcal{O}(p^4)$ strong operators of Gasser-Leutwyler [32] and the N_i 's to the octet $|\Delta S| = 1$ one of Ecker-Kambor-Wyler [33]. The 27-plet counterterms, suppressed by the $\Delta I = 1/2$ rule, are collectively denoted by D_i [6, 34]. The L_i, N_i and D_i occur in separately finite combinations in \hat{c} . Finally, note that the weak mass operator does not contribute. This has to be so since it could not have been absorbed in the weak counterterms $N_{14,15,18}$.

The above loop amplitude induces the following branching fraction for $z > 0.2$:

$$\mathcal{B} (K^+ \rightarrow \pi^+ \gamma \gamma)_{z>0.2}^{L, SU(3), \mathcal{O}(p^4)} = (5.77 + 1.64\hat{c} + 0.29\hat{c}^2) \times 10^{-7}. \quad (65)$$

This expression is not much affected by the momentum cut, as can be inferred from the shape of the two-photon invariant mass spectrum which exhibits the characteristic peak above the $\pi^+ \pi^-$ threshold.

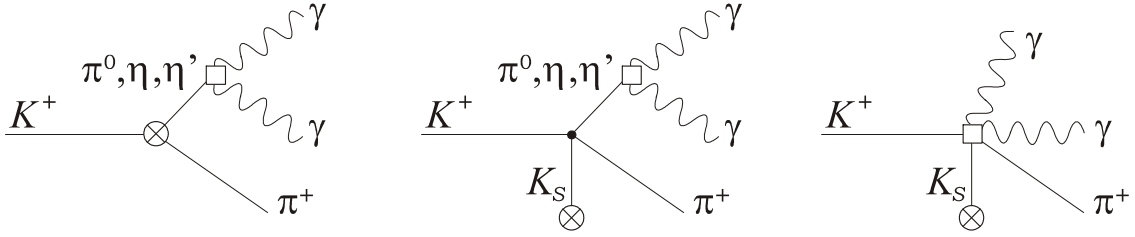


Figure 8: Pole and tadpole diagrams for the process $K^+ \rightarrow \pi^+ \gamma \gamma$.

At $\mathcal{O}(p^6)$, unitarity corrections from $K \rightarrow \pi\pi\pi$ as well as vector meson effects must be included, and were analyzed in Ref. [35]. The former increase the rate by about 30 – 40% while the latter should be smaller. From the corrected spectrum and rate, but assuming negligible pole contributions, a fit to the E787 data [36], (here we quote only the branching fraction)

$$\mathcal{B}(K^+ \rightarrow \pi^+ \gamma \gamma)_{100 \text{ MeV} < P_{\pi^+} < 180 \text{ MeV}}^{\text{exp}} = (6.0 \pm 1.5 \pm 0.7) \times 10^{-7} \quad (66)$$

with $P_{\pi^+} = \frac{M_K}{2} \lambda(1, r_\pi^2, z)^{1/2}$, the π^+ momentum, leads to the $\mathcal{O}(1)$ positive value

$$\hat{c} = 1.8 \pm 0.6. \quad (67)$$

5.2 Pole amplitude in U(3) ChPT

The pole diagrams for $K^+ \rightarrow \pi^+ \gamma \gamma$ are similar to those for $K_S \rightarrow \pi^0 \gamma \gamma$, with in addition a five-particle contact interaction from the WZW term (25) in the case of the weak mass operator Q_8^m (Fig.8). A straightforward leading order computation in $U(3)$ ChPT gives:

$$B(T^2) = \frac{16}{3} (m_K^2 - m_\pi^2) [G_8 B_8(T^2) + G_8^s B_8^s(T^2) + G_{27} B_{27}(T^2)], \quad (68)$$

with

$$B_8(T^2) = \frac{m_0^2 - 10m_K^2 + 3m_\pi^2 + 7T^2}{2(T^2 - m_\eta^2)(T^2 - m_{\eta'}^2)}, \quad B_8^s(T^2) = \frac{-5m_K^2 + 2m_\pi^2 + 3T^2}{(T^2 - m_\eta^2)(T^2 - m_{\eta'}^2)}, \quad (69)$$

$$B_{27}(T^2) = \frac{m_0^2(5m_K^2 - m_\pi^2 - 4T^2) + (15m_K^2 - 7m_\pi^2 - 8T^2)(m_\pi^2 - T^2)}{3(T^2 - m_\pi^2)(T^2 - m_\eta^2)(T^2 - m_{\eta'}^2)}.$$

Again, $m_{\pi, K, \eta, \eta'}$ stand for the theoretical masses, which ensures the absence of Q_8^m effects when the two tadpole graphs are included. Unlike for $K_S \rightarrow \pi^0 \gamma \gamma$, the three pole functions B_8, B_8^s and B_{27} are now independent as \hat{Q}_1, \hat{Q}_2 and \hat{Q}_6 all contribute. Note that the pion pole disappears in B_8 , leaving a constant term, because of the $T^2 - m_\pi^2$ momentum dependence of the off-shell $K^+ \rightarrow \pi^+ \pi^0$ amplitude (purely $\Delta I = 3/2$ once on-shell).

The pole-induced branching fraction as a function of m_0 is depicted in Fig.9a. It is not a monotonically decreasing function down to the $SU(3)$ limit as in the $K_S \rightarrow \pi^0 \gamma \gamma$ case. On the contrary, it exhibits a strong suppression for m_0 between 1.0 and 1.5 GeV. Below 1 GeV, the η pole begins to be felt significantly, hence the rate increases as in Fig.6a.

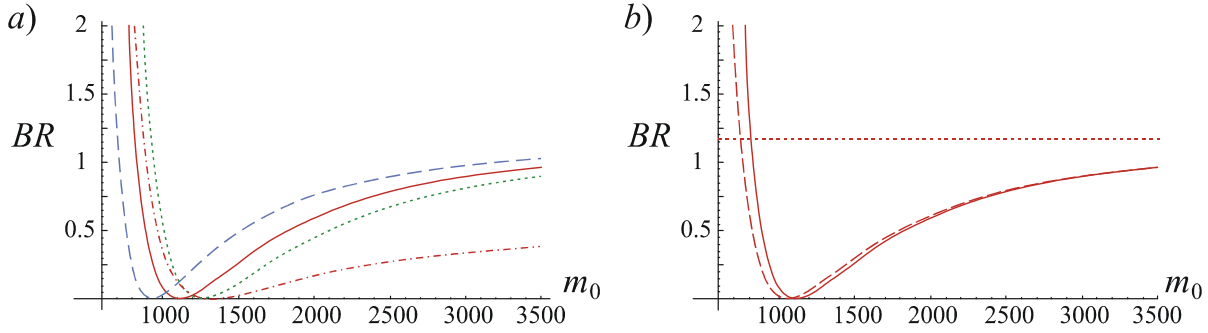


Figure 9: a) $\mathcal{B}(K^+ \rightarrow \pi^+ \gamma \gamma)^{poles}$, $\times 10^7$, as a function of m_0 for $G_8^s/G_8 = -0.3, 0, +0.3$ (dashed, plain, dotted) and for G_8 alone (dash-dotted). b) Comparison between the $\mathcal{O}(p^4)$ $SU(3)$ result (dotted), idem plus the m_0^{-2} corrections (dashed), and full $\mathcal{O}(p^4)$ $U(3)$ result (plain), with $G_8^s = 0$ for the three curves.

5.3 Reduction of the pole amplitude to $SU(3)$ ChPT

The $SU(3)$ limit of the above result can be investigated expanding the pole functions in powers of $1/m_0^2$:

$$\begin{aligned}
B_8(T^2) &= \frac{-1/2}{T^2 - m_{\eta_8}^2} - \frac{4(5m_K^2 - 2m_\pi^2 - 3T^2)(m_K^2 - T^2)}{3(T^2 - m_{\eta_8}^2)^2 m_0^2} + \mathcal{O}(m_0^{-4}), \\
B_8^s(T^2) &= 0 + \frac{5m_K^2 - 2m_\pi^2 - 3T^2}{(T^2 - m_{\eta_8}^2)m_0^2} + \mathcal{O}(m_0^{-4}), \\
B_{27}(T^2) &= \frac{5/4}{T^2 - m_\pi^2} + \frac{1/12}{T^2 - m_{\eta_8}^2} - \frac{2(5m_K^2 - 2m_\pi^2 - 3T^2)(3m_K^2 - m_\pi^2 - 2T^2)}{9(T^2 - m_{\eta_8}^2)^2 m_0^2} + \mathcal{O}(m_0^{-4}),
\end{aligned} \tag{70}$$

The behavior of the total rate as a function of m_0 when the m_0 series is truncated at a given order is displayed in Fig.9b:

- The $\mathcal{O}(p^4)$ $SU(3)$ amplitude (dotted line in Fig.9b) corresponds to the $\mathcal{O}(m_0^0)$ terms [31], and gives

$$\mathcal{B}(K^+ \rightarrow \pi^+ \gamma \gamma)_{z>0.2}^{P,SU(3),\mathcal{O}(p^4)} = 1.17 \times 10^{-7}. \tag{71}$$

This result is to be compared to 0.51×10^{-7} without the G_{27} piece. Such a large effect of the 27 operator (see Fig.9a) has been overlooked previously, and arises from the pion pole, absent from the octet, that compensates for the $\Delta I = 1/2$ suppression over the whole phase-space.

- The m_0^{-2} corrections are the collective effect of the $SU(3)$ counterterms $L_7, N_{13}, L_9^{(6)}$ and $N_1^{(6)}$, when saturated by the η_0 (see appendix, Eqs.(96,97,100)). The series seems not well-behaved in the case of B_8 , again because the leading term is suppressed by the absence of the π^0 pole factor. In particular, for m_0 between 1 GeV and 1.5 GeV, the m_0^{-2} and m_0^0 terms interfere destructively and even cancel each other out for a given T^2 inside the phase-space. This is the origin of the dip shown in Fig.9a, as confirmed by the dashed line in Fig.9b. Said differently, the $\Delta I = 1/2$ enhanced B_8

amplitude, being essentially due to the η_8 pole, is very sensitive to $\eta - \eta'$ mixing effects.

- It is a well-known fact that when the leading order is suppressed for some reason, one can expect sizeable effects from the NLO corrections. Since in the present case the NLO corrections are not suppressed by any mechanism (compare the m_0^{-2} correction in Eqs.(70) and (55)), the series is expected to behave correctly afterwards. The plain line in Fig.9b shows that this is indeed the case: the full $U(3)$ result is rather well reproduced by the m_0^{-2} corrections alone.

Note, finally, that for $m_0 < 1$ GeV, B_8 and B_{27} begin to interfere destructively, instead of constructively in the $SU(3)$ limit.

5.4 Pole contribution to the rate

Given the strong sensitivity of the pole amplitude to the $\eta - \eta'$ system, the prescription Eq.(39) has to be enforced before numerical evaluation. Expressions similar to those of Eq.(58) are then obtained:

$$\begin{aligned}
B_8(T^2) &= \frac{3}{4(M_K^2 - M_\pi^2)} + \frac{2M_K^2 + M_\pi^2 - 3T^2}{4(M_K^2 - M_\pi^2)} \left(\frac{c_\theta c_\eta}{T^2 - M_\eta^2} + \frac{s_\theta c_{\eta'}}{T^2 - M_{\eta'}^2} \right) \\
&\quad - \frac{1}{\sqrt{2}} \left(\frac{s_\theta c_\eta}{T^2 - M_\eta^2} - \frac{c_\theta c_{\eta'}}{T^2 - M_{\eta'}^2} \right), \tag{72} \\
B_8^s(T^2) &= -\frac{3}{2\sqrt{2}} \left(\frac{s_\theta c_\eta}{T^2 - M_\eta^2} - \frac{c_\theta c_{\eta'}}{T^2 - M_{\eta'}^2} \right), \\
B_{27}(T^2) &= \frac{5M_K^2 - 7M_\pi^2 + 2T^2}{4(M_K^2 - M_\pi^2)(T^2 - M_\pi^2)} + \frac{3M_K^2 - M_\pi^2 - 2T^2}{4(M_K^2 - M_\pi^2)} \left(\frac{c_\theta c_\eta}{T^2 - M_\eta^2} + \frac{s_\theta c_{\eta'}}{T^2 - M_{\eta'}^2} \right),
\end{aligned}$$

with $c_\eta \equiv c_\theta - 2\sqrt{2}s_\theta$ and $c_{\eta'} \equiv s_\theta + 2\sqrt{2}c_\theta$, as in Sec.4.3⁵. The pole contribution to the rate as a function of G_8^s/G_8 is depicted in Fig.10b for $z > 0.2$.

In the positive sign alternative for G_8^s/G_8 , it could account for an increase of the total rate by more than 20%, and should be taken into account in the extraction of \hat{c} , Eq.(67). The shape of the differential rate could be affected too, but only mildly, as illustrated for a particular set of parameters in Fig.10a.

Conversely, for the preferred value $G_8^s/G_8 \simeq -1/3$, the pole contribution is completely suppressed (about 10^{-9}). This is a pure numerical coincidence: the three contributions $Q_{8,8s,27}$ are of the same order, but can interfere destructively for $G_8^s/G_8 < 0$. No definite prediction can be made in this case since $\mathcal{O}(p^6)$ corrections can no longer be neglected. Let us thus simply give an upper bound:

$$G_8^s/G_8 = -0.38 \pm 0.12 \Rightarrow \mathcal{B}(K^+ \rightarrow \pi^+ \gamma \gamma)_{z>0.2}^{\text{P},U(3),\mathcal{O}(p^4)} < 0.3 \times 10^{-7}. \tag{73}$$

⁵Note that, for both $K_S \rightarrow \pi^0 \gamma \gamma$ and $K^+ \rightarrow \pi^+ \gamma \gamma$, the two-mixing angle result is immediately obtained by substituting ($f_i = \sec(\theta_0 - \theta_8) F_\pi/F_i$)

$$\begin{aligned}
c_\theta c_{\eta'} &\rightarrow f_0 c_8 (f_8 s_0 + 2\sqrt{2} f_0 c_8), \quad s_\theta c_{\eta'} \rightarrow f_8 s_0 (f_8 s_0 + 2\sqrt{2} f_0 c_8) \\
s_\theta c_\eta &\rightarrow f_0 s_8 (f_8 c_0 - 2\sqrt{2} f_0 s_8), \quad c_\theta c_\eta \rightarrow f_8 c_0 (f_8 c_0 - 2\sqrt{2} f_0 s_8)
\end{aligned}$$

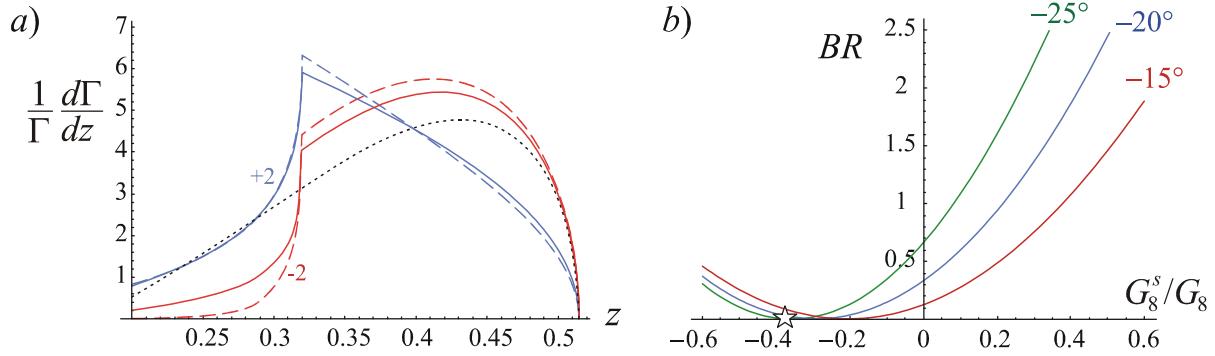


Figure 10: a) $K^+ \rightarrow \pi^+ \gamma \gamma$ normalized differential rate for $\mathcal{O}(p^4)$ loop + pole (plain), loop alone (dashed) and pole alone (dotted) contributions, with $\hat{c} = \pm 2$ and $G_8^s/G_8 = +1/3$, $\theta_P = -20^\circ$. b) $\mathcal{B}(K^+ \rightarrow \pi^+ \gamma \gamma)^{poles}$, $\times 10^7$, as a function of G_8^s/G_8 for $\theta_P = -15^\circ, -20^\circ, -25^\circ$. The star refers to Eq.(23).

This could go up to around 0.5×10^{-7} with $\mathcal{O}(p^6)$ effects but, in any case, no signal of pole contribution should show up experimentally, neither in the total nor in the differential rate.

5.5 Analysis of the low energy end of the $\gamma\gamma$ spectrum

Recently, the E949 Collaboration has obtained the following upper limit [30]:

$$\mathcal{B}(K^+ \rightarrow \pi^+ \gamma \gamma)_{P_{\pi^+} > 213 \text{ MeV}}^{\text{exp}} < 8.3 \times 10^{-9}, \quad (74)$$

assuming a spectrum of the shape predicted by ChPT with unitarity corrections. This corresponds to a $\gamma\gamma$ invariant mass in the range $0 < z < 0.0483$, below the π^0 pole. The loop and pole leading order $SU(3)$ predictions for this range are given by:

$$\mathcal{B}(K^+ \rightarrow \pi^+ \gamma \gamma)_{z < 0.0483}^{\text{L}, SU(3), \mathcal{O}(p^4)} = (0.06\hat{c}^2 + 0.15\hat{c} + 0.09) \times 10^{-9}, \quad (75)$$

$$\mathcal{B}(K^+ \rightarrow \pi^+ \gamma \gamma)_{z < 0.0483}^{\text{P}, SU(3), \mathcal{O}(p^4)} = 1.0 \times 10^{-9}. \quad (76)$$

For \hat{c} of order 1, the loop contribution should be $< 10^{-9}$. Including the unitarity corrections analyzed in Ref. [35], which are specially large for small z , it raises to

$$\mathcal{B}(K^+ \rightarrow \pi^+ \gamma \gamma)_{z < 0.0483}^{\text{L}, SU(3), \text{unitarized}} = 6.1 \times 10^{-9}. \quad (77)$$

A large error (presumably more than 50%) should be assigned to this number given the rather poor theoretical control over this small corner of phase-space.

The pole contribution, including η_0 effects, should also be taken into account. Restricting the phase-space integration to the present range, we find the situation shown in Fig.11. Interestingly, it appears that given the rather large unitarity corrections, and the present experimental bound on the high π^+ momentum end of the spectrum, negative values of G_8^s/G_8 are preferred. Together with the possibility of correlated study of the total and differential rates, this makes of $K^+ \rightarrow \pi^+ \gamma \gamma$ a promising mode to gain information on this ratio.

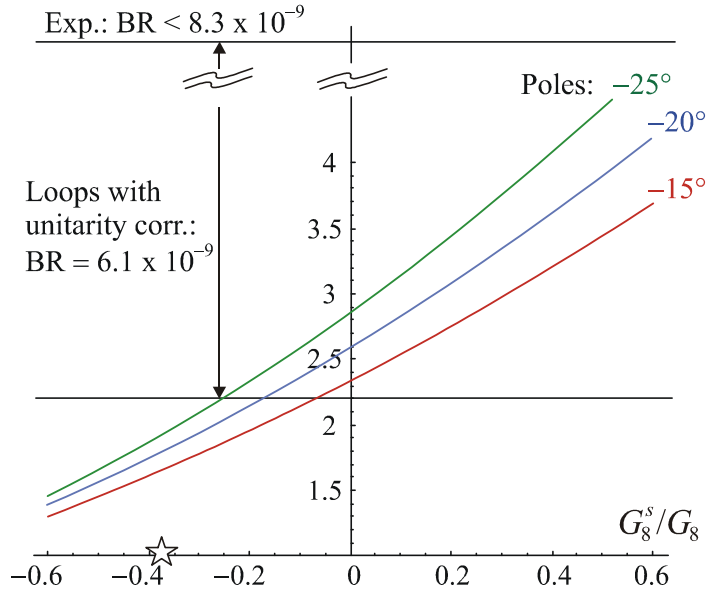


Figure 11: $\mathcal{B}(K^+ \rightarrow \pi^+ \gamma \gamma)^{poles}$ for $z < 0.0483, \times 10^9$. Assuming non-negligible loop contributions [35], the recent upper bound [30] hints towards negative values for G_8^s/G_8 . The star refers to Eq.(23).

6 Other radiative modes

In this section, we consider two other modes involving pole amplitudes. Our discussion will be very brief, because the sensitivity to the parameter of interest G_8^s/G_8 will turn out to be either very suppressed like for $K_L \rightarrow \pi^0 \pi^0 \gamma \gamma$, or buried among other unknown parameters like for $K_L \rightarrow \pi^+ \pi^- \gamma$.

6.1 The $K_L \rightarrow \pi^0 \pi^0 \gamma \gamma$ decay

This process is entirely due to pole diagrams at $\mathcal{O}(p^4)$ (see Fig.12), and was analyzed in $SU(3)$ ChPT in Ref. [37]. The $U(3)$ amplitude is very cumbersome and will not be given explicitly. Its main features are (independently of the use of the physical mass prescription):

- It receives contributions from Q_8, Q_8^s and Q_{27} . As for $K_L \rightarrow \gamma \gamma$, there is no tadpole graph but the contribution of Q_8^m still cancels out when the η, η' theoretical masses are inserted.
- It depends on both the T^2 ($\gamma \gamma$ invariant mass) and Q^2 ($\pi \pi$ invariant mass) kinematical variables, while the $SU(3)$ amplitude depends only on T^2 .
- As for $K_S \rightarrow \pi^0 \gamma \gamma$, the G_8, G_8^s and G_{27} pieces are not independent because the current \times current \hat{Q}_2 operator does not contribute.

At first sight, one could think that the possible double occurrence of the pseudoscalar poles would give a good sensitivity to G_8^s . Unfortunately, this is not the case because the available phase-space for the $\gamma \gamma$ invariant mass is very much concentrated around the π^0 pole. Since

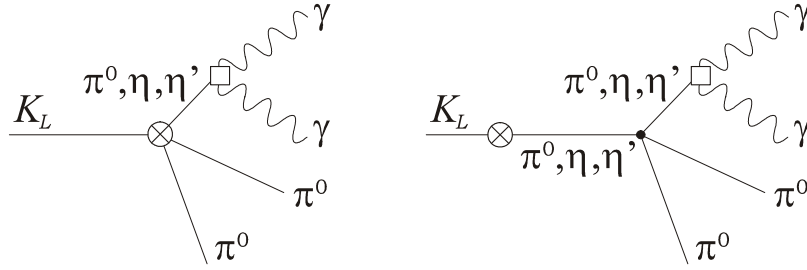


Figure 12: Typical pole diagrams for the process $K_L \rightarrow \pi^0 \pi^0 \gamma \gamma$.

$\eta, \eta' \rightarrow \pi^0 \pi^0 \pi^0$ are both isospin violating, it is then again the π^0 pole that dominates the initial $K_L \rightarrow P$ transition. The effects of the η, η' and G_8^s are thus completely suppressed.

Numerically, we have checked that, indeed, dealing with the mode in $U(3)$ ChPT with the physical mass prescription Eq.(39) changes the $SU(3)$ result of Ref. [37] only at the percent level, no matter the $\gamma\gamma$ invariant mass cuts. In addition, differential rates with respect to either T^2 or Q^2 are only slightly modified. In conclusion, the effects of the η_0 and G_8^s are at the percent level, beyond experimental sensitivity, and also beyond theoretical control since $\mathcal{O}(p^6)$ corrections to the dominant π^0 pole amplitudes are certainly bigger than a few percents.

6.2 The $K_L \rightarrow \pi^+ \pi^- \gamma$ decay

This mode receives many types of contributions, so let us briefly describe its structure. The decay amplitude can be decomposed into electric and magnetic transitions. The electric piece starts at $\mathcal{O}(p^2)$, and is completely determined at this order by the bremsstrahlung from $K_L \rightarrow \pi^+ \pi^-$. It is therefore CP -violating and suppressed. At $\mathcal{O}(p^4)$, there is also a loop contribution, which is quite small [38].

This has allowed experimental access to the magnetic transition [39,40]. This one starts at $\mathcal{O}(p^4)$ with contributions from local $\Delta S = 1$ odd-parity operators ($\sim N_{29} + N_{31}$, see Ref. [38]) and pole diagrams (Fig.13a). In addition, $\mathcal{O}(p^6)$ effects were seen to be important from the experimental observation of a non-zero slope in the photon energy. A detailed study at that order is done in Ref. [41], including both vector meson exchanges and chiral loops, and we will rely on that work for conventions and numerics (as well as for a complete reference list).

In the present work, we wish only to comment on the pole part of the magnetic amplitude (the F_1 piece in Refs. [38,41], shown in Fig.13a), which has been seen to be very sensitive to nonet symmetry breaking [19]. In our framework, this translates into a sensitivity to G_8^s .

As for $K_L \rightarrow \gamma\gamma$, the pole amplitude vanishes in $SU(3)$ at $\mathcal{O}(p^4)$ when enforcing the GMO relation. In $U(3)$, it is simply obtained by substituting $V_{\gamma\gamma}^{\mu\nu}$ in Eq.(32) by

$$V_{\pi^+ \pi^- \gamma}^\mu = -\frac{e}{2\sqrt{2}\pi^2 F^3} \begin{pmatrix} 1 \\ 0 \\ 0 \end{pmatrix} i\varepsilon^{\mu\nu\rho\sigma} p_\nu^{\pi^+} p_\rho^{\pi^-} k_\sigma^\gamma, \quad (78)$$

and thus arises again only through the $\bar{u}u$ component of the weak vertex, i.e. through \hat{Q}_1 . As for $K_L \rightarrow \gamma\gamma$, NLO effects from \hat{Q}_6 are assumed to behave according to usual chiral counting and thus are discarded. Note also that the analysis of $K_L \rightarrow \gamma\gamma$ at $\mathcal{O}(p^6)$ in $SU(3)$ presented in the appendix would not be much modified for the present mode, and that its conclusions are

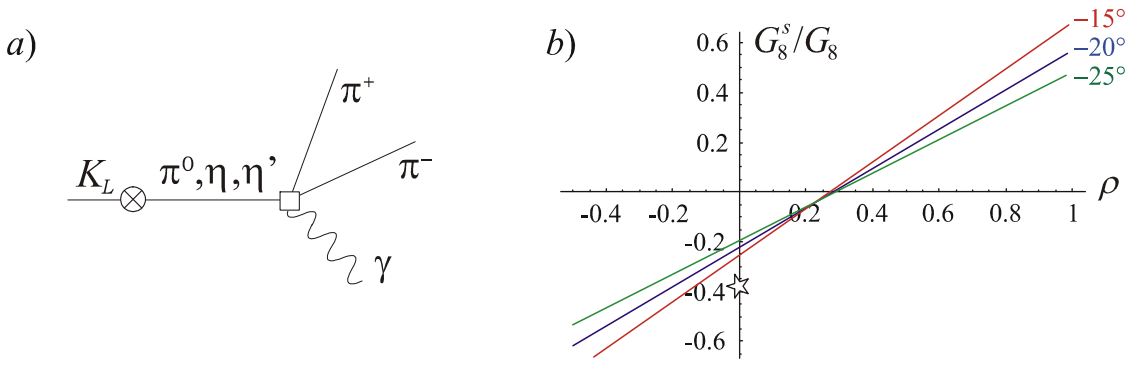


Figure 13: a) Anomalous pole contribution to the magnetic $K_L \rightarrow \pi^+\pi^-\gamma$ amplitude. b) Numerical correspondence between the parameter ρ defined in [41] and G_8^s/G_8 (see text). The star refers to Eq.(23).

still valid. For these reasons, the phenomenological pole parametrization of F_1 usually adopted is not appropriate and should be replaced by

$$F_1 = -\frac{G_8^s + \frac{2}{3}G_{27}}{G_8} M_K^2 \left(\frac{1}{M_K^2 - M_\pi^2} + \frac{(c_\theta - \sqrt{2}s_\theta)^2}{3(M_K^2 - M_\eta^2)} + \frac{(s_\theta + \sqrt{2}c_\theta)^2}{3(M_K^2 - M_{\eta'}^2)} \right), \quad (79)$$

which has no G_8 contribution, is now dominated by the η pole and is thus negative when $G_8^s/G_8 < 0$.

Instead of repeating the numerical analysis of Ref. [41], we have chosen to simply give a dictionary relating their parameter ρ to the ratio G_8^s/G_8 for fixed F_1 (Fig.13b). In other words, to each value of F_1 corresponds a given ρ in Ref. [41], and a given G_8^s in Eq.(79), which are then reported in Fig.13b. It is important to understand that this is only a numerical equivalence, and does not correspond to the analytic equivalence of Eq.(49) (for example, $G_8^s/G_8 = -1/3$ implies $\rho \simeq 0.5$ via Eq.(49), but is accounted for by the smaller effective value $\rho = -0.15 \pm 0.07$ in Fig.13b). As already explained in Sec.3.4, the usual phenomenological pole model is incorrect because not proportional to $\rho - 1$ (to a good approximation).

Unfortunately, in Ref. [41], ρ was only marginally allowed into negative territory because this was believed to be in contradiction with $K_L \rightarrow \gamma\gamma$. As we have seen, $K_L \rightarrow \gamma\gamma$ points towards $G_8^s/G_8 \simeq -1/3$, and therefore negative values of ρ should be allowed. From the fits of Ref. [41], it seems that such values could accommodate the data, but additional work would be needed. In any case, it is clear that a precise extraction of G_8^s/G_8 from $K_L \rightarrow \pi^+\pi^-\gamma$ would be quite intricate due to the presence of many counterterms and vector meson couplings whose estimations introduce some amount of model dependence.

7 Compatibility with hadronic observables

This final section concerns non-radiative observables. First, we will see how our understanding of $K_L \rightarrow \gamma\gamma$ can help estimating the $\mathcal{O}(G_F^2)$ $K_L - K_S$ mass difference generated by pseudoscalar pole contributions. Then, we will turn to the direct CP-violating parameter ε'/ε , and analyze how the information gained on the $\Delta I = 1/2$ rule fits in the usual theoretical analysis.

7.1 Pole contributions to ΔM_{LS}

Experimentally, the $K_L - K_S$ mass difference, $\Delta M_{LS} \equiv M(K_L) - M(K_S)$, is quite well-known [24]

$$\Delta M_{LS}^{\text{exp}} = (3.483 \pm 0.006) \times 10^{-12} \text{ MeV} . \quad (80)$$

Unfortunately, theoretical control on $\Delta M_{LS} \sim 2 \text{Re} \langle K^0 | \mathcal{H}_W | \bar{K}^0 \rangle$ is a long-standing issue since both short-distance and long-distance contributions are present [42]

$$\Delta M_{LS} = \Delta M_{LS}^{SD} + \Delta M_{LS}^{LD} . \quad (81)$$

The first piece, from W -box diagrams with virtual c, t quarks, accounts for the bulk of the experimental value, $\Delta M_{LS}^{SD} / \Delta M_{LS}^{\text{exp}} = (86 \pm 26) \%$ [43] (see also [44]). The second one arises from W -box diagrams with low-virtuality u quarks, hence has to be dealt with light meson exchanges. In the present work, we will concentrate on the long-distance, non-local contributions from double insertion of $|\Delta S| = 1$ transitions (see for example [42, 45]).

In $SU(3)$ ChPT, only pole and tadpole diagrams (Fig.14a) occur at $\mathcal{O}(p^2)$, giving rise to the $\mathcal{O}(G_F^2)$ mass difference:

$$\Delta M_{LS}^{\text{pole}} \stackrel{SU(3)}{=} 2F^4 m_K^3 (G_{27} - G_8 + G_8^m)^2 \left(\frac{1}{m_K^2 - m_\pi^2} + \frac{1/3}{m_K^2 - m_{\eta_8}^2} \right) . \quad (82)$$

Though both $M(K_L)$ and $M(K_S)$ are renormalized by a term in $(G_8^m)^2$ from the tadpole diagrams (Fig.14a)⁶, the mass difference is independent of G_8^m as can be seen by enforcing the GMO relation (29). Still, everything cancels along with it, and ΔM_{LS}^{LD} exactly vanishes.

Pseudoscalar poles thus begin to contribute at $\mathcal{O}(p^4)$ in $SU(3)$, through loop corrections to the masses and weak vertices, along with genuine two-pseudoscalar loops, $K \rightarrow PP \rightarrow \bar{K}$, from which they cannot be disentangled. Overall, these $\mathcal{O}(p^4)$ loops require some unknown $\mathcal{O}(p^4)$ local counterterms, including $|\Delta S| = 2$ ones, to cancel their divergence (see the comment at the end of the appendix). Alternatively, as they correspond to the low-energy tail of the W -box diagrams, an approximate matching with short-distance can be implemented [46].

Performing the same analysis in $U(3)$ has the immediate advantage that the transition $s\bar{d} \rightarrow \bar{u}u \rightarrow \bar{s}d$ is caught at leading order (Fig.14b). Adapting Eq.(32), with $V_{\gamma\gamma}^{\mu\nu}$ replaced by V_{weak} , we reach

$$\Delta M_{LS}^{\text{pole}} \stackrel{U(3)}{=} \frac{-12F^4 m_K^3}{m_0^2 - 3m_K^2 + 3m_\pi^2} \left(G_8^s + \frac{2}{3}G_{27} \right)^2 = \frac{-12F^4 m_K^3}{m_0^2 - 3m_K^2 + 3m_\pi^2} (G_W x_1)^2 . \quad (83)$$

Though Q_8 and Q_8^m cancel again upon enforcing the theoretical $\eta_0 - \eta_8$ mass matrix (31), the non-zero contribution from $(\hat{Q}_1)^2$ survives (neglecting \hat{Q}_3 and \hat{Q}_5). As for $K_L \rightarrow \gamma\gamma$, \hat{Q}_2 and \hat{Q}_6 cannot contribute at leading order (such a disappearance of \hat{Q}_6 has already been noticed in Ref. [20]). The physical mass prescription is then used to restore correct analytical properties, but only for the $(\hat{Q}_1)^2$ contribution

$$\Delta M_{LS}^{\text{pole}} = 2F^4 M_K^3 \left(G_8^s + \frac{2}{3}G_{27} \right)^2 \left(\frac{1}{M_K^2 - M_\pi^2} + \frac{(c_\theta - \sqrt{2}s_\theta)^2}{3(M_K^2 - M_\eta^2)} + \frac{(s_\theta + \sqrt{2}c_\theta)^2}{3(M_K^2 - M_{\eta'}^2)} \right) . \quad (84)$$

⁶In the usual language (see Ref. [5]), this is a manifestation of the necessary realignment of the vacuum brought by the tadpole operator Q_8^m . As a result, at $\mathcal{O}(G_F^2)$, the physical $K_{L,S}$ masses are free parameters, and only the mass difference is calculable.

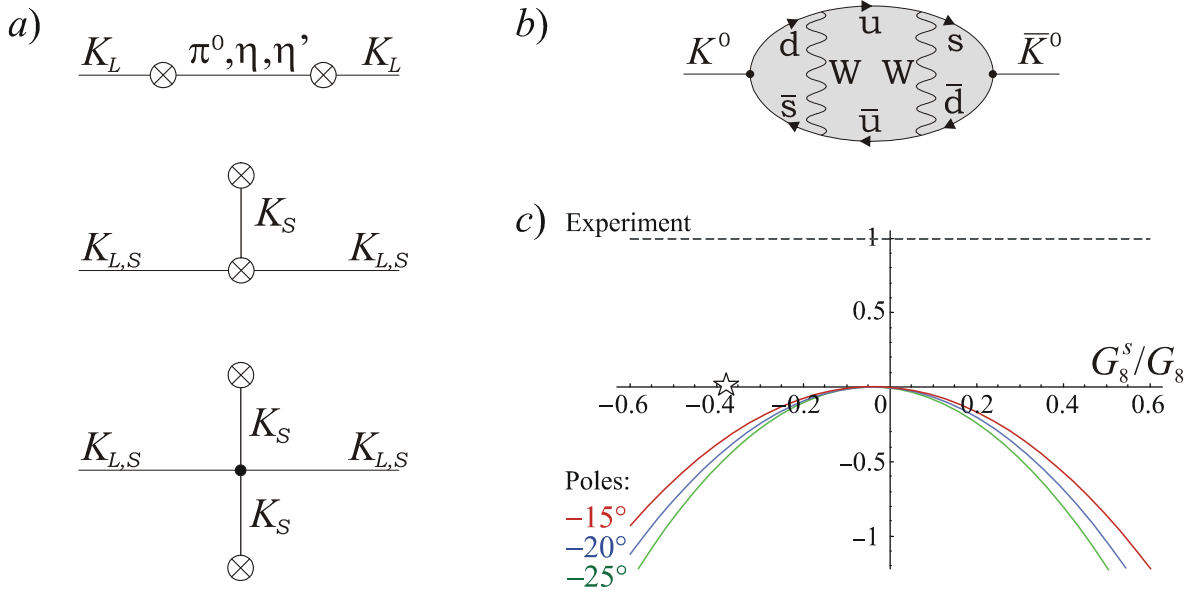


Figure 14: a) Pole and tadpole diagrams for ΔM_{LS}^{LD} . b) Long-distance $\bar{u}u$ contribution. c) Fraction of pole contribution to $\Delta M_{LS}^{\text{exp}}$ as a function of G_8^s/G_8 for $\theta_P = -15^\circ, -20^\circ, -25^\circ$. The star refers to Eq.(23).

Once again, the η contribution dominates such that poles give a negative contribution to ΔM_{LS} , which grows (quasi) quadratically with G_8^s/G_8 (Fig.14c). Note also the similarity of Eq.(84) with Eq.(79), stemming from the proportionality of the vertices $V_{\pi^+\pi^-\gamma}^\mu$ (78) and V_{weak} (35) when $x_6 \rightarrow 0$.

To reach Eq.(84), we have discarded x_6 because it does not occur at lowest order, i.e. in Eq.(83). As explained in Sec. 3, in such cases, the physical mass prescription would generate some contributions corresponding to the inclusion of only a small class of higher order effects, and pole amplitudes being plagued by cancellations, this is a very dangerous procedure. In the case of the $K_L \rightarrow \gamma\gamma$ (and $K_L \rightarrow \pi^+\pi^-\gamma$) radiative mode, we went on by arguing that \hat{Q}_6 is in fact suppressed at higher order because the quantum numbers of the initial K_L together with the electromagnetic WZW vertex project out non- $\bar{u}u$ transitions, and kept only the \hat{Q}_1 contribution in our comparison with experiment.

This last step cannot be extended to ΔM_{LS} since there is no such projection from CP-symmetry and charge conservation for the $K^0 - \bar{K}^0$ transition. In particular, the $(\hat{Q}_6)^2$ contribution at $\mathcal{O}(p^4)$ is certainly not small now since it contains part of the $K \rightarrow PP \rightarrow \bar{K}$ loops, i.e. the low-energy tail of the box diagram depicted in Ref. [46]. These loops give a positive contribution to ΔM_{LS} , and though their estimates vary greatly, they are generally of a few tens of percent of $\Delta M_{LS}^{\text{exp}}$.

Eq.(84) is therefore the correct leading order estimation for the long-distance $(\hat{Q}_1)^2$ piece only. To compare it with experiment, let us take, with respect to $\Delta M_{LS}^{\text{exp}}$, the conservative upper bound of +50% for the $K \rightarrow PP \rightarrow \bar{K}$ loops, assuming they saturate the $(\hat{Q}_6)^2$ contribution, and +150% for the short-distance piece. We can then safely infer from Fig.14c that pole contributions

should be no less than -100% , i.e.

$$|G_8^s/G_8| < 0.6 . \quad (85)$$

Furthermore, for our preferred value $G_8^s/G_8 \simeq -1/3$, poles contribute for about -30% such that the long-distance contributions partially cancel each other.

7.2 Strong penguin contribution to ε'/ε

The direct CP-violation observable ε'/ε is related to the imaginary part of the $K \rightarrow \pi\pi$ isospin amplitudes, and additional theoretical inputs are necessary. We do not intend to give a full account of ε'/ε theory (for recent theoretical updates and references, see [47]), but would like to see if the large penguin contribution to the $\Delta I = 1/2$ rule found at the hadronic scale is compatible with the small ε'/ε observed [48–51]

$$\left(\frac{\varepsilon'}{\varepsilon}\right)_{\text{exp}} = (1.67 \pm 0.16) \times 10^{-3} . \quad (86)$$

The general formula for this quantity is, in terms of the isospin amplitudes defined in Eq.(16),

$$\frac{\varepsilon'}{\varepsilon} = e^{i\Phi} \frac{\omega}{\sqrt{2}|\varepsilon|} \left[\frac{\text{Im } A_2}{\text{Re } A_2} - \frac{\text{Im } A_0}{\text{Re } A_0} \right] \quad \text{with } \Phi = -\delta + \frac{\pi}{4} \approx 0 . \quad (87)$$

We will concentrate on the strong QCD penguin contribution, and thus discard isospin breaking effects due to $\pi^0 - \eta^{(\prime)}$ and electroweak penguins. Keeping then only the $\text{Im } A_0/\text{Re } A_0$ part, we get in terms of matrix elements of the dominant Q_1, Q_2 and Q_6 four-quark operators

$$\left(\frac{\varepsilon'}{\varepsilon}\right)_0 = \frac{\omega}{\sqrt{2}|\varepsilon|} \frac{\text{Im } \lambda_t}{\text{Re } \lambda_u} \frac{3y_6(\mu) \langle Q_6(\mu) \rangle_0}{-z_1(\mu) \langle Q_1(\mu) \rangle_0 + 2z_2(\mu) \langle Q_2(\mu) \rangle_0 + 3z_6(\mu) \langle Q_6(\mu) \rangle_0} , \quad (88)$$

with $\langle Q_i \rangle_0 \equiv \langle \pi\pi (I=0) | Q_i | K \rangle$ and $\lambda_i \equiv V_{id}V_{is}^*$.

At this level, the usual treatment consists in taking the experimental value for the denominator (i.e. $\text{Re } A_0$), and trying to modelize the $Q_6(\mu)$ matrix element in the numerator at a scale for which $y_6(\mu)$ is calculable. In this respect, the penguin fraction \mathcal{F}_P does not help much since running it up to $\mu > 1$ GeV throughout the non-perturbative regime is beyond our reach. Alternatively, to make use of the extra theoretical and phenomenological information $\mathcal{F}_P \simeq 2/3$, see Fig.4, let us rewrite Eq.(88) in a way independent of the hadronic matrix elements [52]

$$\left(\frac{\varepsilon'}{\varepsilon}\right)_0 = \frac{\omega}{\sqrt{2}|\varepsilon|} \frac{\text{Im } \lambda_t}{\text{Re } \lambda_u} \mathcal{F}_P \frac{y_6(\mu_{\text{hadr}})}{z_6(\mu_{\text{hadr}})} \quad (89)$$

with μ_{hadr} the typical scale of ChPT. The difficulty now is shifted from getting up to $\langle Q_6(\mu) \rangle$ in the perturbative regime, to getting down to the ratio $y_6(\mu)/z_6(\mu)$ in the non-perturbative regime.

From the experimental constraints on the CKM factors λ_i , it follows

$$\left(\frac{\varepsilon'}{\varepsilon}\right)_0 \simeq 5 \mathcal{F}_P \frac{y_6(\mu_{\text{hadr}})}{z_6(\mu_{\text{hadr}})} \left(\frac{\varepsilon'}{\varepsilon}\right)_{\text{exp}} . \quad (90)$$

Allowing for at most a 50% reduction due to isospin breaking effects, we obtain then

$$\frac{1}{5} \lesssim \mathcal{F}_P \frac{y_6(\mu_{\text{hadr}})}{z_6(\mu_{\text{hadr}})} \lesssim \frac{2}{5} . \quad (91)$$

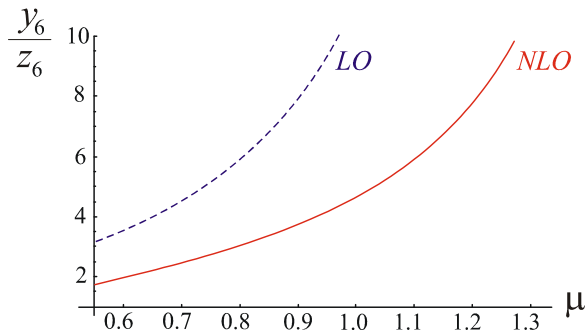


Figure 15: The running of the ratio $y_6(\mu)/z_6(\mu)$ at leading and next-to-leading logarithmic approximation, in the \overline{MS} / NDR scheme, for $\alpha_S(M_Z) = 0.118$, $m_c = 1.3$ GeV (based on [2]).

For $\mathcal{F}_P \simeq 2/3$, this range is by no means unrealistic. As shown in Fig.15, the ratio $y_6(\mu)/z_6(\mu)$ exhibits a scale dependence (this is obvious since $z_6(m_c) = 0$ at LO), which quickly decreases with μ [2]. This behavior arises because at both LO and NLO in the NDR scheme, $y_6(\mu) - z_6(\mu)$ is scale independent to better than 10% for μ even as low as 0.6 GeV where clearly perturbation theory should no longer be trusted. It is therefore possible that though $y_6(\mu_{hadr})$ and $z_6(\mu_{hadr})$ are completely beyond our reach, their ratio could be controlled. If, for once in the long story of ε'/ε , nature was kind enough to somehow protect the specific ratio $y_6(\mu)/z_6(\mu)$, an alternative theoretical strategy would be revived. This remains to be seen though all we can say (on the basis of Fig.15) is that a value smaller than one for this ratio is certainly not ruled out, and would require the bound

$$G_8^s/G_8 > -0.8, \quad (92)$$

which is not much more constraining than what would have been obtained from the QCD-inspired analysis of Sec.2.3 (see Fig.1), i.e. $G_8^s/G_8 > -1$.

8 Conclusion

A number of radiative K decays involving pseudoscalar pole diagrams have been investigated in the context of large- N_c ChPT. Emphasis has been laid on the $\Delta S = 1$ weak operator Q_8^s , peculiar to the $U(3)$ framework, that holds the key to a better understanding of the underlying flavor-changing mechanisms and, in particular, to a phenomenological extraction of the penguin contribution to the $\Delta I = 1/2$ rule. Let us now summarize our results, divided into three categories:

Phenomenological constraints on the weak coupling G_8^s from radiative K decays

- The $K_L \rightarrow \gamma\gamma$ decay turns out to be mainly driven by the nonet-symmetry breaking operators Q_8^s and Q_{27} (i.e., \hat{Q}_1), and dominated by the η pole. The contribution of Q_8 (i.e., \hat{Q}_6) is suppressed by large cancellations. Experimental data then imply $G_8^s/G_8 \simeq \pm 1/3$. The analysis of $K_L \rightarrow \gamma\gamma^*$ of Ref. [25] favors the negative solution. This sign is important for the interference between the short-distance and dispersive $\gamma\gamma$ contributions to $K_L \rightarrow \mu^+\mu^-$ [18, 53].

- The $K_S \rightarrow \pi^0 \gamma \gamma$ rate is enhanced by η_0 effects for most values of G_8^s/G_8 . In addition, the fact that neither the shape of the $m_{\gamma\gamma}$ spectrum nor the rate for low $m_{\gamma\gamma}$ are affected by G_8^s could be exploited to disentangle the NLO effects (like vector resonances) from the η_0 ones, and to achieve a clean extraction of G_8^s/G_8 .
- In the case of $K^+ \rightarrow \pi^+ \gamma \gamma$, the pole contribution to the total rate is negligible with respect to loops for $G_8^s/G_8 < 0$, but can be as large as 20% for $G_8^s/G_8 > 0$ (poles are then needed to extract \hat{c}). This situation arises from the fact that the G_8 , G_8^s and G_{27} pole contributions are of the same order. At the low energy end of the $\gamma\gamma$ spectrum, the recent experimental upper bound [30] points towards $G_8^s/G_8 < 0$ (still, theoretical uncertainties are large in this small corner of phase-space).
- The effects of η, η' and G_8^s on $K_L \rightarrow \pi^0 \pi^0 \gamma \gamma$ have proved negligible.
- Relying on Ref. [41], the $K_L \rightarrow \pi^+ \pi^- \gamma$ data are found compatible with a large range of G_8^s/G_8 values. A precise extraction seems beyond reach given the many unknown phenomenological parameters.
- The pole contributions to ΔM_{LS}^{LD} were also briefly discussed. As for $K_L \rightarrow \gamma \gamma$, they arise from Q_8^s and Q_{27} (i.e., \hat{Q}_1^2). Yet, this time, non-negligible Q_8 (i.e., \hat{Q}_6^2) effects are expected at NLO from the presence of $K \rightarrow PP \rightarrow \bar{K}$ loops. The poles result in a negative contribution to ΔM_{LS} , while loop and short-distance W -box diagram contributions are positive. Conservative bounds on the latter two lead to $|G_8^s/G_8| < 0.6$. For $G_8^s/G_8 \simeq -1/3$, large cancellations are expected between the loop and pole long-distance contributions.

QCD-inspired operator basis and the penguin contribution to the $\Delta I = 1/2$ rule

- The three weak operators (Q_8, Q_8^s, Q_{27}) of $U(3)$ ChPT can be related to the low-energy realizations of the current-current and penguin operators ($\hat{Q}_1, \hat{Q}_2, \hat{Q}_6$). QCD-inspired theoretical expectations then lead to the range $(G_8^s/G_8)_{th} = -0.38 \pm 0.12$, compatible with all the phenomenological constraints given above. The non-perturbative evolution of current-current operators is therefore rather smooth, while the \hat{Q}_6 penguin is significantly enhanced, and responsible for about 2/3 of the $\Delta I = 1/2$ rule at the hadronic scale. This large penguin fraction is compatible with the small ε'/ε observed, though a significant cancellation with isospin breaking effects might be welcome.
- For $K_L \rightarrow \gamma \gamma$, $K_L \rightarrow \pi^+ \pi^- \gamma$ and ΔM_{LS}^{LD} , the well-known vanishing of pole contributions at lowest order in $SU(3)$ ChPT and the subsequent pathological sensitivity to NLO effects are explained. Indeed, the transitions $K_L \rightarrow \bar{u}u \rightarrow \gamma \gamma / \pi^+ \pi^- \gamma / K_L$, i.e. through Q_1 , cannot be caught in $SU(3)$ at LO simply because there are not enough independent weak operators. This does not occur in $U(3)$, where the $\bar{u}u$ leading order effect can be identified. Contributions from NLO (in particular from the $\bar{d}d, \bar{s}s$ transitions driven by Q_6) should then behave according to chiral counting, except for ΔM_{LS}^{LD} where $K \rightarrow PP \rightarrow \bar{K}$ loops are present.

- We have proposed a two-step procedure to deal with pole amplitudes: first, the identification of vanishing contributions through the enforcement of theoretical masses (i.e., working consistently at a given order), then the restoration of correct analytical properties by setting the poles at their right places for the remaining contributions only.
- The weak mass term Q_8^m has been shown to disappear in all the modes considered, in both $SU(3)$ and $U(3)$ ChPT, as long as one is working consistently at a given order (see above). This is non-trivial since pole amplitudes involve both off-shell weak transitions [28] and the WZW action.
- The connection between $U(3)$ and $SU(3)$ ChPT has been analyzed in details for all modes and, though sometimes large, η_0 effects are not incompatible with naive $SU(3)$ ChPT power counting. Indeed, they can be reproduced, to a good approximation, with four $SU(3)$ NLO counterterms saturated by η_0 exchanges. For $K_L \rightarrow \gamma\gamma$, a complete analysis at $\mathcal{O}(p^6)$ has been presented, showing in particular that decay constant corrections do not occur, and that saturating the $K_L \rightarrow \gamma\gamma$ amplitude with \hat{Q}_1 amounts essentially to assume that a combination of scalar-dominated counterterms is small.

In conclusion, a consistent picture seems to emerge from our analysis. In particular, naive expectations from QCD are already well-supported by phenomenological constraints. Additional experimental information from radiative K decays are eagerly awaited, as they could give further insight into the interplay between strong and weak interactions at low energies.

Acknowledgments: C.S. and S.T. are pleased to thank Gino Isidori for numerous discussions and encouragements. Also, they acknowledge the many useful interactions with participants of the LNF Spring School, LNF Spring Institute and Kaon 2005 International Workshop, where parts of this work were presented. J.-M. G. thanks Gino Isidori and Giulia Pancheri for their kind hospitality during his visit at the Laboratori Nazionali di Frascati. Many thanks also to Ulrich Nierste for sharing with us his updated value of ΔM_{LS}^{SD} .

C.S. and S.T. are supported by IHP-RTN, EC contract No. HPRN-CT-2002-00311 (EURIDICE). J.-M. G. acknowledges support by the Belgian Federal Office for Scientific, Technical and Cultural Affairs through the Interuniversity Attraction Pole P5/27.

Appendix: $K_L \rightarrow \gamma\gamma$ in $SU(3)$ ChPT at $\mathcal{O}(p^6)$

In the text, we argued that corrections to the weak vertices $K_L \rightarrow \pi^0, \eta_8$, to the π^0, η_8 propagators and to the $\pi^0, \eta_8 \rightarrow \gamma\gamma$ vertices (in particular through $F \rightarrow F_\pi, F_{\eta_8}$) should either reconstruct the dominant $\bar{s}d(\bar{d}s) \rightarrow \bar{u}u \rightarrow \gamma\gamma$ transition, or vanish (to a large extent). This is a strong statement since it implies a very specific interplay between the weak and strong sectors of $SU(3)$ ChPT, and between $\mathcal{O}(p^4)$ and $\mathcal{O}(p^6)$ counterterms. It is the purpose of this appendix to check this assertion by performing the full calculation of $K_L \rightarrow \gamma\gamma$ in $SU(3)$ ChPT at $\mathcal{O}(p^6)$. In particular, we will detail all the cancellations occurring between the various corrections depicted in Fig.16.

Full $\mathcal{O}(p^6)$ amplitude

From the diagrams of Fig.16, summing over the π^0 and η_8 poles, we obtain:

$$\mathcal{A}^{\mu\nu}(K_L \rightarrow \gamma\gamma) = \frac{m_K^2 \alpha}{8\pi^3 F} [\mathcal{F}] i\varepsilon^{\mu\nu\rho\sigma} k_{1\rho} k_{2\sigma}, \quad (93)$$

with

$$\begin{aligned} \mathcal{F} = & - \left(G_8 + \frac{2}{3} G_{27} \right) \frac{A_K - A_\pi}{m_K^2 - m_\pi^2} \\ & - G_8 \left[1024\pi^2 \left(2L_7 + L_8 + \frac{L_8^{(6)} + 6L_9^{(6)}}{9} + \frac{2N_{12} + 2N_{13} - N_6}{8} + \frac{N_1^{(6)}}{12} + N_i^{(6)} \right) \right] \\ & + G_{27} \left[1024\pi^2 \left(2L_7 + L_8 + \frac{L_8^{(6)} + 6L_9^{(6)}}{9} + D_i + D_i^{(6)} \right) \right] \\ & + G_8^m \left[1024\pi^2 \left(2L_7 + L_8 + \frac{L_8^{(6)} + 6L_9^{(6)}}{9} \right) \right], \quad (94) \end{aligned}$$

$A_i = m_i^2(D_\varepsilon - \log m_i^2/\mu^2 + 1)$ and $D_\varepsilon = \frac{2}{\varepsilon} - \gamma + \log 4\pi$. We have used the standard basis of Gasser-Leutwyler [32] for the $\mathcal{O}(p^4)$ strong counterterms (L_i) and the Ecker-Kambor-Wyler [33] one for the $\mathcal{O}(p^4)$ octet $\Delta S = 1$ counterterms (N_i). In the third diagram, the CT (counterterm) contribution originates from the odd-parity $\mathcal{O}(p^6)$ strong Lagrangian, which is written in the Ebertshauser-Fearing-Scherer [54] or Bijnens-Girlanda-Talavera [55] basis (up to an overall normalization):

$$\mathcal{O}_8^{EFS} = \mathcal{O}_7^{BGT} = \frac{1}{(4\pi F)^2} L_8^{(6)} i\varepsilon_{\mu\nu\alpha\beta} \langle \chi_- f_+^{\mu\nu} f_+^{\alpha\beta} \rangle, \quad (95)$$

$$\mathcal{O}_9^{EFS} = \mathcal{O}_8^{BGT} = \frac{1}{(4\pi F)^2} L_9^{(6)} i\varepsilon_{\mu\nu\alpha\beta} \langle \chi_- \rangle \langle f_+^{\mu\nu} f_+^{\alpha\beta} \rangle, \quad (96)$$

with $\chi_\pm \equiv U\chi^\dagger \pm \chi U^\dagger$, $f_\pm^{\mu\nu} \equiv F_L^{\mu\nu} \pm UF_R^{\mu\nu}U^\dagger$ (in our case $\chi = rM$ with M the light quark mass matrix, $F_L^{\mu\nu} = F_R^{\mu\nu} = -eQF^{\mu\nu}$ with $F^{\mu\nu}$ the QED field strength tensor and Q the light quark charge matrix). In the last diagram, the CT contribution originates from the odd-parity $\mathcal{O}(p^6)$ weak Lagrangian. To our knowledge, no operator basis has been set up for it yet. For the purpose of the present analysis, only one of the direct $K_L \rightarrow \gamma\gamma$ couplings will be needed explicitly:

$$\mathcal{O}_{|\Delta S|=1}^{(6)} = \frac{G_8}{2(4\pi)^2} N_1^{(6)} i\varepsilon_{\mu\nu\alpha\beta} \langle \lambda_6 \chi_- \rangle \langle f_+^{\mu\nu} f_+^{\alpha\beta} \rangle. \quad (97)$$

All the others are collectively denoted by $N_i^{(6)}$ (octet part). Note that the $\mathcal{O}(p^4)$ CTs L_i and N_i alone suffice to absorb the G_8 part of the loop divergence, $L_i^{(6)}$ and $N_i^{(6)}$ being thus separately finite. Finally, also the 27-plet CTs, though needed for renormalization, will not be specified explicitly, and are collectively denoted by D_i [6, 34] and $D_i^{(6)}$.

Note also that, to reach Eq.(94), the initial K_L mass M_K^2 has been expressed back in terms of the bare mass m_K^2 (see Ref. [32]). Alternatively, the weak rotation can be performed to discard the $K_L \rightarrow \pi^0, \eta_8$ $\mathcal{O}(p^2)$ vertices [27, 31].

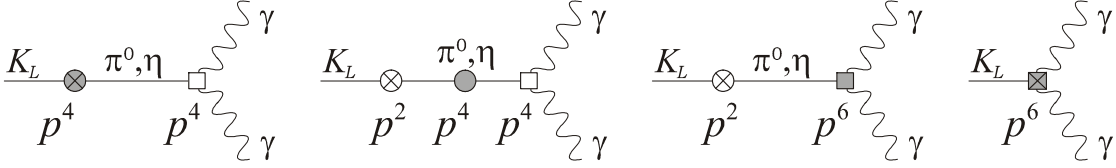


Figure 16: $K_L \rightarrow \gamma\gamma$ at $\mathcal{O}(p^6)$. Grey vertices stand for local counterterms and meson loops.

Discussion of the counterterms

A first encouraging observation is that many counterterms drop out when summing over the π^0 and η_8 poles ($N_{5,8,10,11}$ and $L_{4,5,6}$) or taking the external particles on-shell (like N_{29}, N_{31}), while the final combination of chiral logs is very simple and very small (it vanishes for $\mu \sim 550$ MeV). In particular, the a priori significant correction due to $SU(3)$ breaking effects in the decay constants (i.e., $L_{4,5}$) drops out, the impact of $F_{\eta_8}/F_\pi \neq 1$ being thus at least of $\mathcal{O}(p^8)$. But this is not the end of the story: there are still many interplays between the counterterms, though it is necessary to go beyond the strict $SU(3)$ framework to get hold of them.

As is well-known [32], L_7 is well-described by a tree-level η_0 exchange, which gives it an abnormal counting $L_7 \sim N_c^2$ (still, see the discussion in [56]). In the same way, N_{13} , $L_9^{(6)}$ and $N_1^{(6)}$ (which also have zero anomalous dimensions) can be saturated by the η_0 resonance, surviving then as well in the large- N_c limit. The explicit reductions of the $U(3)$ weak operators to $SU(3)$ read ($\bar{\eta}_0 \equiv \sqrt{2/3}\eta_0/F$)

$$\begin{aligned} Q_8 &= 4 [\langle \lambda_6 L_\mu L^\mu \rangle - F^2 \langle \lambda_6 L_\mu \rangle (D^\mu \bar{\eta}_0)] , \\ Q_8^s &= -6F^2 \langle \lambda_6 L_\mu \rangle (D^\mu \bar{\eta}_0) , \\ Q_8^m &= F^4 [\cos(\bar{\eta}_0) \langle \lambda_6 \chi_+ \rangle + i \sin(\bar{\eta}_0) \langle \lambda_6 \chi_- \rangle] , \end{aligned} \quad (98)$$

where the left-hand side $\in U(3)$ and the right-hand side $\in SU(3)$ (Q_{27} does not couple to the singlet). Similarly, the WZW $U(3)$ Lagrangian is reduced as [57]

$$\mathcal{L}_{WZW}^{U(3)} = \mathcal{L}_{WZW}^{SU(3)} + \frac{iN_c}{288\pi^2} \varepsilon_{\mu\nu\alpha\beta} \left[\frac{3}{4} \langle f_+^{\mu\nu} f_+^{\alpha\beta} \rangle + \frac{1}{4} \langle f_-^{\mu\nu} f_-^{\alpha\beta} \rangle + i \langle D^\mu U D^\nu U^\dagger f_+^{\alpha\beta} \rangle \right] \langle i\bar{\eta}_0 \rangle . \quad (99)$$

A straightforward computation then gives

$$\begin{aligned} L_7 &= -\frac{N_c F^2}{144m_0^2}, & N_{13} &= \frac{N_c F^2}{18m_0^2} \left(1 + \frac{3G_8^s}{2G_8} - \frac{G_8^m}{G_8} \right) , \\ L_9^{(6)} &= -\frac{N_c^2 F^2}{144m_0^2}, & N_1^{(6)} &= \frac{N_c^2 F^2}{18m_0^2} \left(1 + \frac{3G_8^s}{2G_8} - \frac{G_8^m}{G_8} \right) \end{aligned} \quad (100)$$

after partial integration and use of the $SU(3)$ equations of motion. Note that other counterterms (like N_{24} , $L_7^{(6)}$, $L_{11}^{(6)}$, ...) could be saturated by the η_0 , but none contributing for on-shell photons.

Besides, we will set $L_8^{(6)} = 0$, as suggested by the success of the LO description of $\pi^0 \rightarrow \gamma\gamma$. There is then only the $L_9^{(6)}$ counterterm for $\eta \rightarrow \gamma\gamma$ at $\mathcal{O}(p^6)$ (chiral loops and wavefunction renormalization amount to $F \rightarrow F_{\eta_8}$, see Ref. [58]). Using its η_0 -saturated value with $m_0 \simeq 850$ MeV, we obtain $\Gamma(\eta \rightarrow \gamma\gamma) \simeq 0.4$ keV, instead of 0.1 keV without $L_9^{(6)}$. Experimentally,

$\Gamma(\eta \rightarrow \gamma\gamma) = (0.510 \pm 0.026) \text{ keV}$ [24], which means that $L_9^{(6)}$ indeed accounts for the bulk of NLO effects. This is simply a manifestation of the fact that $U(3)$ at LO reproduces $\eta, \eta' \rightarrow \gamma\gamma$ reasonably well without extra operators like Eq.(26).

Inserting the values (100) in Eq.(94), we find that the G_8 and G_8^m pieces of the η_0 -saturated CTs indeed cancel out, leaving only a term proportional to $G_8^s + \frac{2}{3}G_{27}$:

$$\begin{aligned} \mathcal{F} = & -128\pi^2 \left(G_8^s + \frac{2}{3}G_{27} \right) \frac{F^2}{m_0^2} + \text{chiral logs} \\ & - 1024\pi^2 \left[G_8 \left(L_8 + \frac{2N_{12} - N_6}{8} + N_i^{(6)} \right) - G_{27} \left(L_8 + D_i + D_i^{(6)} \right) - G_8^m (L_8) \right]. \end{aligned} \quad (101)$$

Note that the use of the $U(3)$ lowest order constraint $F = F_\pi = F_{\eta_0}$ does not affect the observed cancellation since any deviation of F_{η_0}/F_π from unity can be accounted for by varying m_0^2 (saturation from tree-level exchanges).

The first term is of course exactly the $U(3)$ result in the limit $m_0 \rightarrow \infty$ and corresponds to the \hat{Q}_1 contribution, i.e. to the transition $\bar{s}d(\bar{d}s) \rightarrow \bar{u}u \rightarrow \gamma\gamma$. The G_{27} piece ($D_i, D_i^{(6)}$) is suppressed by the $\Delta I = 1/2$ rule and can be discarded, along with the small chiral logs. The remaining $\mathcal{O}(p^4)$ counterterms N_6, N_{12} and L_8 can in principle give a large contribution to $K_L \rightarrow \gamma\gamma$ because of their large numerical coefficients. Still, they all arise from scalar exchanges [33, 59] and it is reasonable to assume that they will behave similarly to the counterterms saturated by pseudoscalar exchanges, i.e. cancel among themselves to a large extent, or act as a correction to the leading \hat{Q}_1 piece. As a further clue, note that there must be some interplay between L_8 and $N_{6,12}$ in order to absorb the contribution of G_8^m in the N_i 's. Finally, the fate of the remaining $\mathcal{O}(p^6)$ local $K_L \rightarrow \gamma\gamma$ counterterms ($N_i^{(6)}$) is not clear, but it is at least possible that they are small.

In conclusion, we have pin-pointed the combination of counterterms on which we make an assumption when we saturate the $K_L \rightarrow \gamma\gamma$ rate by the \hat{Q}_1 contribution. We hope that some further work will be able to get at least an upper bound on this combination, so that the precise measurements of $K_L \rightarrow \gamma\gamma$ (27) will reliably fix G_8^s/G_8 . For now, as explained in the text, there are other theoretical and phenomenological indications that G_8^s/G_8 has a value around $-1/3$, which then unambiguously implies that the remaining CTs in Eq.(101) must at least partially cancel among themselves.

Comments on ΔM_{LS}

Finally, let us make a few comments on the similar computation for ΔM_{LS}^{LD} . As explained in the text, in $SU(3)$ at $\mathcal{O}(p^4)$, there are both corrections to the pole amplitudes, similar to the $K_L \rightarrow \gamma\gamma$ ones given in Eq.(94), and pseudoscalar loops like $K \rightarrow PP \rightarrow \bar{K}$. Large cancellations among corrections are again observed, in particular among those for the decay constants and masses. It should be noted also that though the terms in $G_8^m G_{8,27}$ and $(G_8^m)^2$ are non-local for $M(K_L)$ and $M(K_S)$ (i.e., contain some chiral logs), they appear only locally for ΔM_{LS}^{LD} (i.e., they are proportional to $\mathcal{O}(p^4)$ counterterms and can thus be absorbed in the N_i 's). As at $\mathcal{O}(p^2)$, only the mass difference is unambiguous in Chiral Perturbation Theory (see Sec.7.1).

Concerning the reconstruction of the \hat{Q}_1 contribution, the role of $L_9^{(6)}$ and $N_1^{(6)}$ is taken up by the $\Delta S = 2$ counterterm $\langle \lambda_6 \chi_- \rangle^2$, saturated by the η_0 . Again, L_7, N_{13} and this $\Delta S = 2$ counterterm appear initially with a complicated coefficient involving G_8^2 , but they conspire to reconstruct the $s\bar{d} \rightarrow \bar{u}u \rightarrow \bar{s}d$ transition, i.e. a term with the coefficient $(G_8^s + 2G_{27}/3)^2$. At this

stage, an expression similar to Eq.(101) is reached, but with in addition some $K \rightarrow PP \rightarrow \bar{K}$ loop functions (and divergences), and a correspondingly different combination of the remaining counterterms.

In conclusion, because of the presence of $K \rightarrow PP \rightarrow \bar{K}$ loops and $\Delta S = 2$ counterterms, it does not appear possible to get extra information from ΔM_{LS}^{LD} on the counterterms remaining for $K_L \rightarrow \gamma\gamma$ in Eq.(101). Still, the interplays among corrections leading to the reconstruction of the \hat{Q}_1 contribution are found to occur also for ΔM_{LS} .

References

- [1] M. K. Gaillard and B. W. Lee, Phys. Rev. Lett. **33** (1974) 108; G. Altarelli and L. Maiani, Phys. Lett. **B52** (1974) 351; A. I. Vainshtein, V. I. Zakharov and M. A. Shifman, JETP **45** (1977) 670; F. J. Gilman and M. B. Wise, Phys. Rev. **D20** (1979) 2392.
- [2] G. Buchalla, A. J. Buras and M. E. Lautenbacher, Rev. Mod. Phys. **68** (1996) 1125.
- [3] E. Witten, Nucl. Phys. **B156** (1979) 269.
- [4] P. Di Vecchia and G. Veneziano, Nucl. Phys. **B171** (1980) 253; C. Rosenzweig, J. Schechter and C. G. Trahern, Phys. Rev. **D21** (1980) 3388; E. Witten, Annals Phys. **128** (1980) 363; K. Kawarabayashi and N. Ohta, Nucl. Phys. **B175** (1980) 477.
- [5] C. Bernard, T. Draper, A. Soni, H. Politzer and M. Wise, Phys. Rev. **D32** (1985) 2343; R. J. Crewther, Nucl. Phys. **B264** (1986) 277; M. Leurer, Phys. Lett. **B201** (1988) 128.
- [6] J. Kambor, J. Missimer and D. Wyler, Nucl. Phys. **B346** (1990) 17.
- [7] R. S. Chivukula, J. M. Flynn and H. Georgi, Phys. Lett. **B171** (1986) 453.
- [8] W. A. Bardeen, A. J. Buras and J.-M. Gérard, Phys. Lett. **B180** (1986) 133.
- [9] W. A. Bardeen, A. J. Buras and J.-M. Gérard, Nucl. Phys. **B293** (1987) 787; Phys. Lett. **B192** (1987) 138.
- [10] J. P. Fatelo and J.-M. Gérard, Phys. Lett. **B347** (1995) 136.
- [11] J. Wess and B. Zumino, Phys. Lett. **B37** (1971) 95; E. Witten, Nucl. Phys. **B223** (1983) 422.
- [12] H. Leutwyler, Nucl. Phys. Proc. Suppl. **64** (1998) 223; R. Kaiser, *Diploma work*, University of Bern (1997).
- [13] A. Lai *et al.* [NA48 Collaboration], Phys. Lett. **B551** (2003) 7.
- [14] M. Adinolfi *et al.* [KLOE Collaboration], Phys. Lett. **B566** (2003) 61.
- [15] M. K. Gaillard and B. W. Lee, Phys. Rev. **D10** (1974) 897.
- [16] E. Ma and A. Pramudita, Phys. Rev. **D24** (1981) 2476.
- [17] L. L. Chau and H. Y. Cheng, Phys. Rev. Lett. **54** (1985) 1768; J. F. Donoghue, B. R. Holstein and Y.-C. R. Lin, Nucl. Phys. **B277** (1986) 650; J. L. Goity, Z. Phys. **C34** (1987) 341; J. L. Goity and L. Z. Zhang, Phys. Lett. **B398** (1997) 387.

- [18] D. Gomez Dumm and A. Pich, Phys. Rev. Lett. **80** (1998) 4633.
- [19] H. Y. Cheng, Phys. Lett. **B245** (1990) 122.
- [20] A. J. Buras and J.-M. Gérard, Nucl. Phys. **B264** (1986) 371.
- [21] J.-M. Gérard and E. Kou, Phys. Lett. **B616** (2005) 85.
- [22] R. Escribano and J. M. Frère, JHEP **0506** (2005) 029.
- [23] F. Ambrosino *et al.* [KLOE Collaboration], *hep-ex/0508027*.
- [24] S. Eidelman *et al.* [Particle Data Group], Phys. Lett. **B592**, 1 (2004) and 2005 partial update for the 2006 edition available on the PDG WWW pages (URL: <http://pdg.lbl.gov/>).
- [25] G. D'Ambrosio and J. Portolés, Nucl. Phys. **B492** (1997) 417.
- [26] A. Lai *et al.* [NA48 Collaboration], Phys. Lett. **B578** (2004) 276.
- [27] G. Ecker, A. Pich and E. de Rafael, Phys. Lett. **B189** (1987) 363.
- [28] J. Bijnens, E. Pallante and J. Prades, Nucl. Phys. **B521** (1998) 305.
- [29] G. Buchalla, G. D'Ambrosio and G. Isidori, Nucl. Phys. **B672** (2003) 387.
- [30] A. V. Artamonov *et al.* [E949 Collaboration], *hep-ex/0505069*.
- [31] G. Ecker, A. Pich and E. de Rafael, Nucl. Phys. **B303** (1988) 665.
- [32] J. Gasser and H. Leutwyler, Annals Phys. **158** (1984) 142; Nucl. Phys. **B250** (1985) 465.
- [33] G. Ecker, J. Kambor and D. Wyler, Nucl. Phys. **B394** (1993) 101.
- [34] G. Esposito-Farese, Z. Phys. **C50** (1991) 255.
- [35] G. D'Ambrosio and J. Portolés, Phys. Lett. **B386** (1996) 403; erratum *ibid.*, **B389** (1996) 770.
- [36] P. Kitching *et al.* [E787 Collaboration], Phys. Rev. Lett. **79** (1997) 4079.
- [37] H. Dykstra, J. M. Flynn and L. Randall, Phys. Lett. **B270** (1991) 45; R. Funck and J. Kambor, Nucl. Phys. **B396** (1993) 53.
- [38] G. Ecker, H. Neufeld and A. Pich, Nucl. Phys. **B413** (1994) 321.
- [39] E. J. Ramberg *et al.* [E731 Collaboration], Phys. Rev. Lett. **70** (1993) 2525.
- [40] A. Alavi-Harati *et al.* [KTeV Collaboration], Phys. Rev. Lett. **86** (2001) 761.
- [41] G. D'Ambrosio and J. Portoles, Nucl. Phys. **B533** (1998) 523.
- [42] L. Wolfenstein, Nucl. Phys. **B160** (1979) 501; C. Hill, Phys. Lett. **B97** (1980) 275.
- [43] S. Herrlich and U. Nierste, Phys. Rev. **D52** (1995) 6505; U. Nierste, private communication.
- [44] O. Cata and S. Peris, JHEP **0407** (2004) 079.

- [45] J. F. Donoghue, E. Golowich and B. R. Holstein, Phys. Lett. **B135** (1984) 481; I. I. Bigi and A. I. Sanda, Phys. Lett. **B148** (1984) 205; P. Cea and G. Nardulli, Phys. Lett. **B152** (1985) 251; M. R. Pennington, Phys. Lett. **B153** (1985) 439; M. Neubert, Z. Phys. **C50** (1991) 243; V. Antonelli, S. Bertolini, M. Fabbrichesi and E. I. Lashin, Nucl. Phys. **B493** (1997) 281.
- [46] J. Bijnens, J.-M. Gérard and G. Klein, Phys. Lett. **B257** (1991) 191; J.-M. Gérard, Acta Phys. Polon. **B21** (1990) 257.
- [47] A. J. Buras and M. Jamin, JHEP **0401** (2004) 048; A. Pich, proceedings of 32nd International Conference on High-Energy Physics (ICHEP 04), Beijing, China, 16-22 Aug 2004, *hep-ph/0410215*.
- [48] A. Alavi-Harati *et al.* [KTeV Collaboration], Phys. Rev. **D67** (2003) 012005; Phys. Rev. Lett. **83** (1999) 22.
- [49] J. R. Batley *et al.* [NA48 Collaboration], Phys. Lett. **B544** (2002) 97; A. Lai *et al.* [NA48 Collaboration], Eur. Phys. J. **C22** (2001) 231; V. Fanti *et al.* [NA48 Collaboration], Phys. Lett. **B465** (1999) 335.
- [50] H. Burkhardt *et al.* [NA31 Collaboration], Phys. Lett. **B206** (1988) 169; G. D. Barr *et al.* [NA31 Collaboration], Phys. Lett. **B317** (1993) 233.
- [51] L. K. Gibbons *et al.* [E731 Collaboration], Phys. Rev. Lett. **70** (1993) 1203.
- [52] F. J. Gilman and M. B. Wise, Phys. Lett. **B93** (1980) 129; Phys. Rev. **D27** (1983) 1128; Phys. Rev. **D20** (1979) 2392.
- [53] G. Isidori and R. Unterdorfer, JHEP **0401** (2004) 009.
- [54] T. Ebertshauser, H. W. Fearing and S. Scherer, Phys. Rev. **D65** (2002) 054033.
- [55] J. Bijnens, L. Girlanda and P. Talavera, Eur. Phys. J. **C23** (2002) 539.
- [56] S. Peris and E. de Rafael, Phys. Lett. **B348** (1995) 539.
- [57] R. Kaiser and H. Leutwyler, Eur. Phys. J. **C17** (2000) 623.
- [58] J. F. Donoghue, B. R. Holstein and Y.-C. R. Lin, Phys. Rev. Lett. **55** (1985) 2766; J. Bijnens, A. Bramon and F. Cornet, Phys. Rev. Lett. **61** (1988) 1453.
- [59] G. Ecker, J. Gasser, A. Pich and E. de Rafael, Nucl. Phys. **B321** (1989) 311.